THE DETAILS OF TURBULENT MIXING PROCESS AND THEIR SIMULATION

Harry E.A. Van den Akker*

Department of Multi-Scale Physics, Faculty of Applied Sciences, Delft University of Technology, Delft, The Netherlands

*Corresponding author E-mail: H.E.A.vandenAkker@TNW.TUDelft.nl

Advances in Chemical Engineering, vol. 31
ISSN 0065-2377
DOI 10.1016/S0065-2377(06)31003-4

Abstract

This chapter is devoted to turbulent mixing processes carried out in - mainly - stirred vessels. It reviews first a number of turbulent flow characteristics as far as relevant to a wide variety of single-phase and two-phase mixing processes and, secondly and most importantly, the details of the advanced Computational Fluid Dynamics (CFD) techniques required for simulating such processes with a large degree of confidence. The processes considered comprise blending, solids suspension, dissolution, precipitation, crystallization, chemical reactions, and dispersing gases and immiscible liquids.

The emphasis in this chapter is on the fruitful application of Large Eddy Simulations for reproducing the local and transient flow conditions in which these processes are carried out and on which their performance depends. In addition, examples are given of using Direct Numerical Simulations of flow and transport phenomena in small periodic boxes with the view to find out about relevant details of the local processes. Finally, substantial attention is paid throughout this chapter to the attractiveness and success of exploiting lattice-Boltzmann techniques for the more advanced CFD approaches.

I. Introduction

Mixing is an operation inherent to numerous processes encountered in the chemical process industries. Mixing devices such as stirred tanks occur abundantly in plants and processing facilities. This review focuses on stirred vessels being operated under turbulent-flow conditions. Their design and scale-up, their operation, and their often seemingly conflicting performances under varying

conditions have always troubled plant engineers and fascinated researchers. The turbulent-flow phenomena and mixing rates encountered in stirred vessels as well as the processes being dependent on proper and effective mixing have been the subject of numerous research studies since the early 1950s (e.g., Rushton *et al*., 1950; Kramers *et al*., 1953).

The early studies often documented Power Number–*Reynolds* Number relationships and related to mixing and circulation times (Holmes *et al*., 1964; Voncken *et al*., 1964). Many scale-up rules in terms of nondimensional numbers were derived for a variety of operations such as blending, aeration (Westerterp *et al*., 1963), and suspending solids (Zwietering, 1958), usually on the basis of integral investigations for specific stirrer/vessel combinations. One was just interested in the global flow field characteristics and in the overall performance of the stirred vessel as a whole. This already was a major step forward in comparison with the fiction of a continuous stirred tank (reactor) widely used in the field of chemical engineering.

Current industrial interests, however, are far beyond this basic level of understanding. Companies are continuously looking for process improvements and for options of debottlenecking plants, in the context of improving performance, profitability, competitiveness, and sustainability. The result is an increasing demand on *local* flow information since in real life many processes exhibit substantial spatial variations in, e.g., bubble or drop size (Tsouris and Tavlarides, 1994; Luo and Svendsen, 1996; Schulze *et al*., 2000; Venneker *et al*. 2002) or in crystal size (Ten Cate *et al*., 2000; Hollander *et al*., 2001a,b; Rielly and Marquis, 2001). Further, the yield and selectivity of many chemical reactors may depend on the rate the various chemical species involved are brought into intimate contact and this rate may vary spatially as well (Bakker and Fasano, 1993; Bakker, 1996; Akiti and Armenante, 2004).

Such spatial variations in, e.g., mixing rate, bubble size, drop size, or crystal size usually are the direct or indirect result of spatial variations in the turbulence parameters across the flow domain. Stirred vessels are notorious indeed, due to the wide spread in turbulence intensity as a result of the action of the revolving impeller. Scale-up is still an important issue in the field of mixing, for at least two good reasons: first, usually it is not just a single nondimensional number that should be kept constant, and, secondly, average values for specific parameters such as the specific power input do not reflect the wide spread in turbulent conditions within the vessel and the nonlinear interactions between flow and process. Colenbrander (2000) reported experimental data on the steady drop size distributions of liquid–liquid dispersions in stirred vessels of different sizes and on the response of the drop size distribution to a sudden change in stirred speed.

Knowledge of spatial variations in bubble, drop, and crystal sizes is often desired or required, but extremely hard to obtain experimentally. Intrusive measuring and sampling probes may disturb flow and process locally. Taking samples may affect the sizes: in the sampling procedure, samples may experience

flow conditions different from those at the sampling position as a result of which particle size may change. Optical techniques may provide a solution but under specific conditions (optical accessability and density) and in specific geometries only. Knowledge of local flow variables and local mixing and transfer rates is hard to obtain experimentally as well, since the turbulent flow in most stirred vessels in industry is inhomogeneous and often time dependent, and comprises a wide range of spatial scales and associated temporal scales.

CFD might provide a way of elucidating all these spatial variations in flow conditions, in species concentrations, in bubble drop and particle sizes, and in chemical reaction rates, provided that such computational simulations are already capable of reliably reproducing the details of turbulent flows and their dynamic effects on the processes of interest. This Chapter reviews the state of the art in simulating the details of turbulent flows and turbulent mixing processes, mainly in stirred vessels. To this end, the topics of turbulence and CFD both need a separate introduction.

A. The Role of Turbulence

The spatial scales in turbulent mixing range from the size of the impeller (blade) down to the typical size of the smallest, so-called *Kolmogorov* eddies in which the turbulent kinetic energy is dissipated into heat due to the action of friction. In many applications, mixing at the small scales is of paramount importance since many rate-limiting phenomena take place within these *Kolmogorov* scale and are dominated by the dynamics of these *Kolmogorov* eddies. Kresta and Brodkey (2004) present a valuable discussion on the role of turbulence in mixing applications and on the role of time and length scales and of scale-up rules. One could say that in turbulent mixing the details really matter! Deriving local rates of energy dissipation within these *Kolmogorov* eddies from experimental velocity data is at its best a tedious activity not viable for chemical engineers in industry. Computational simulations may provide a way out.

The turbulent-flow structures in stirred tanks are highly 3-D and complex because of the complex geometry of the device. Vortical structures, high turbulence levels, and high rates of energy dissipation particularly in the vicinity of the impeller dominate the turbulent flow in stirred tanks. Under the action of the revolving impeller, the fluid is circulated through the tank. Baffles along the tank wall prevent the liquid from carrying out a solid-body rotation about the impeller axis and enhance mixing, partly via vessel-size macroinstabilities. Turbulent flows in stirred vessels are very complex indeed.

As a result, the turbulent-flow field in a stirred vessel may be far from isotropic and homogeneous. Some of the cornerstones of turbulence theory, however, start from the assumption that production and dissipation of turbulent kinetic energy balance *locally*. In many chemical engineering flows, this

assumption may not be satisfied everywhere. In the complex flows of most process equipment, turbulence intensity and other turbulence properties vary spatially. These spatial variations may induce flows, diffusion, and dispersion across the flow domain (see, e.g., Ducci and Yianneskis, 2006). This implies that turbulence is not necessarily dissipated where it has been produced: it first may be transported toward another part of the flow domain to get dissipated there. As a result, strictly speaking, the common concepts of turbulence theory may not be valid and applicable.

Turbulence research still focuses on canonical cases of high *Reynolds* Number flows in order to deepen their understanding of the subject (''the most important unsolved problem of classical physics'', according to the great physicist Richard Feynman). Typical examples are grid/isotropic turbulence (in the absence of walls), channel and pipe flow, and free shear layers and jets (see, e.g., Dimotakis, 2005) or rather simple hydraulic problems (Rodi, 1984). At the same time, turbulence research usually refrains from considering practical chemical engineering problems such as the complications and practicalities of stirred vessels.

Chemical engineers, however, have to find practical ways for dealing with turbulent flows in flow devices of complex geometry. It is their job to exploit practical tools and find practical solutions, as spatial variations in turbulence properties usually are highly relevant to the operations carried out in their process equipment. Very often, the effects of turbulent fluctuations and their spatial variations on these operations are even crucial. The classical toolbox of chemical engineers falls short in dealing with these fluctuations and its effects. Computational Fluid Dynamics (CFD) techniques offer a promising alternative approach.

B. The Role of Computational Fluid Dynamics

Nowadays, the effects of, e.g., vessel design and operation conditions can be assessed by means of computational simulations indeed. To mention just a few examples: standard CFD simulations of stirred vessels are perfectly suited to sort out the effect of varying impeller clearance in terms of eliminating dead zones or reducing their size, or the effect of impeller speed on the degree of solids suspension. Various commercial software vendors offer efficient CFD packages, which in many cases can be seen as real workhorses for industrial applications. CFD has tempestuously developed into a very versatile tool, not only in the hands of fluid flow experts, but also in those of chemical engineers.

Since computational resources have increased substantially at sharply decreasing costs, detailed computational information about the flows can nowadays be obtained even at a fraction of the cost of the corresponding experiments. Consequently, computational modeling of the flow has become an attractive alternative route of describing flows and improving and scaling up operations in stirred tanks. Papers such as Ditl and Rieger (2006) presenting

design correlations drafted on the basis of experimental data collected in long series of tests will soon be a thing of the past.

In the meantime, CFD can even do more. It may be easier to 'measure' the local and transient details of the turbulent flows in stirred vessels and the spatial distributions in, e.g., mixing rates and bubble, drop, and crystal sizes computationally than by means of experimental techniques! A good example is the spatial distribution of the kinetic energy dissipation rate ε (see Micheletti *et al.*, 2004). Such a quest—from commercial interests (*market pull*)—in the details of turbulent flows and associated processes then urges for really powerful CFD techniques. On the reverse, the expectations as to the potential of pursuing a computational route toward a better understanding of turbulent flows and processes are also fed by the remarkable progress made recently in the field of CFD (*technology push*).

This paper deals with the advanced CFD of turbulent stirred vessels. The advances attained in recent years in the field of CFD really matter for the degree of accuracy and confidence at which the performance of stirred reactors and of other operations carried out in stirred vessels can be simulated, as these processes and operations may strongly depend on the details of the physics and chemistry involved. The latter details require the more advanced CFD techniques indeed.

Recently, Paul *et al.* (2004) compiled many engineering design principles developed in the field of mixing over the last 30 years into the NAMF (North American Mixing Forum) Handbook of Mixing. This 'Bible of Mixing' provides within its 1,375 pages a wealth of information and design guidelines for the practicing engineer who needs to both identify and solve mixing problems. It also contains a few chapters and sections reviewing achievements and promises of CFD for the field of mixing. In Chapter 5, Marshall and Bakker (2004) present an overview on Computational Fluid Mixing; their review, however, is rather limited in scope and in computational methods covered. Patterson *et al.* (2004) devote some 30% of their Chapter 13 to computational simulations of 'Mixing and Chemical Reactions.' In the remaining Chapters of the Handbook, CFD is largely presented as an immature technique which may become relevant for the practicing engineer in due course only.

The present author thinks one can and should be much more positive about the merits of CFD so far and about the term at which CFD will replace and improve existing mixing correlations. This message was already passed on at earlier occasions (Van den Akker, 1997, 2000). Substantial progress has been made in exploiting CFD not just for simulating the turbulent-flow field but also with the view of representing the various processes carried out in stirred vessels. Owing to the enormous growth in computer power and the proliferation of models and numerical methods, CFD nowadays is very powerful and versatile. This does not mean that every flow or process can be mimicked in all detail, since Direct Numerical Simulations (DNS) resolving all turbulent fluctuations involved in flow and process will keep requiring insurmountable amounts of

computer power and simulation times for the next decades. Current computer power, however, already offers various ways out which are of inestimable value to practicing engineers indeed.

First of all, the increased computer power makes it possible to switch to transient simulations and to increase spatial resolution. One no longer has to be content with steady flow simulations on relatively coarse grids comprising 10^4–10^5 nodes. Full-scale Large Eddy Simulations (LES) on fine grids of 10^6–10^7 nodes currently belong to the possibilities and deliver realistic reproductions of transient flow and transport phenomena. Comparisons with quantitative experimental data have increased the confidence in LES. The present review stresses that this does not only apply to the hydrodynamics but relates to the physical operations and chemical processes carried out in stirred vessels as well. Examples of LES-based simulations of such operations and processes are due to Hollander *et al.* (2001a,b, 2003), Venneker *et al.* (2002), Van Vliet *et al.* (2005, 2006), and Hartmann *et al.* (2006).

A further option is to forget about simulating the flow and the processes in the whole vessel and to zoom into local processes by carrying out a DNS for a small box. The idea is to focus on the flow and transport phenomena within such a small box, such as mass transport and chemical reactions in or around a few eddies or bubbles, or the hydrodynamic interaction of a limited number of bubbles, drops, and particles including their readiness to collisions and coalescence. Examples of such detailed studies by means of DNS are due to Ten Cate *et al.* (2004) and Derksen (2006b).

The effect of this small box being immersed in the dynamic ambiance of the turbulent flow is mimicked by using periodic boundary conditions, which protect the inside of the box against restricting effects of the boundaries. By imposing typical (averaged) conditions of, e.g., flow, rate of energy dissipation, temperature, species concentrations, and/or volume fractions, we then are capable of studying how the flow and the various processes of interest evolve as a result of the governing models and equations. Where experimental techniques often fail in elucidating the mechanisms behind certain phenomena and processes, computational simulations are perfectly capable of doing this. This is a most welcome aspect of computational simulations indeed.

As a matter of fact, one may think of a multiscale approach coupling a macroscale simulation (preferably, a LES) of the whole vessel to meso or microscale simulations (DNS) of local processes. A rather simple, *off-line* way of doing this is to incorporate the effect of microscale phenomena into the full-scale simulation of the vessel by means of phenomenological coefficients derived from microscale simulations. Kandhai *et al.* (2003) demonstrated the power of this approach by deriving the functional dependence of the single-particle drag force in a swarm of particles on volume fraction by means of DNS of the fluid flow through disordered arrays of spheres in a periodic box; this functional dependence now can be used in full-scale simulations of any flow device.

One may object that such computational simulations are too advanced and too much time consuming for practicing engineers. Similar doubts as to the usefulness of CFD for chemical engineers were raised in the early days of CFD. Nowadays, however, CFD software is used throughout the chemical process industries for a wide variety of applications indeed. This is at least partly due to the development of very versatile and robust commercial CFD software that has turned into a valuable tool for chemical engineers in industry. In addition, in the last 15 years, the size of the computational simulations has increased substantially, keeping more or less equal pace with Moore's law saying the number of transistors on integrated circuits doubles every 2 years. There is no reason why computer power and CFD—in a type of playing leapfrog process—would not keep growing at the same pace. This means that what is advanced and time consuming today will be a routine job in 3 or 5 years. Of course, academia may have the lead in this development.

C. The Scope of this Review

This review paper is restricted to stirred vessels operated in the turbulent-flow regime and exploited for various physical operations and chemical processes. The developments in the field of computational simulations of stirred vessels, however, are not separated from similar developments in the fields of, e.g., turbulent combustion, flames, jets and sprays, tubular reactors, and multiphase reactors and separators. Fortunately, there is a strong degree of synergy and mutual cross-fertilization between these various fields. This review paper focuses on aspects specific to stirred vessels (such as the revolving impeller, the resulting strong spatial variations in turbulence properties, and the macroinstabilities) and on the processes carried out in them.

Because of the above interactions, it is impossible to distinctly mark the start of the CFD of stirred vessels. The first papers on CFD simulations of stirred vessels were due to Harvey and Greaves (1982), Placek and Tavlarides (1985), Placek *et al.* (1986), Middleton *et al.* (1986), and Ranade *et al.* (1989). Patterson was certainly one of the pioneers exploring the options for computational simulations of turbulent reactors (see, e.g., Patterson, 1985). From about 1990 onwards, the triennial European Conferences on Mixing, the bi-annual meetings of the NAMF and the regular IChemE Fluid Mixing Events provided the floor for numerous oral presentations on computational simulations in the mixing field as well as for beneficial exchanges of ideas between academic researchers and industrial users.

The results of some of the early simulations in the field of stirred vessels are still reported in this review paper. They may serve to illustrate the substantial progress made since the early days. Several of the strong simplifications of those days are no longer required indeed. Most importantly, incorporating physical

operations and chemical processes into the fluid flow simulations has become quite viable, as this review intends to demonstrate.

This review strongly focuses on the potential of LES and DNS for reproducing not only the hydrodynamics of turbulent stirred vessels but also for providing a basis for simulating a wide variety of physical and chemical processes in this equipment. The first journal paper presenting simulation results obtained by means of LES for a stirred vessel was due to Eggels (1996), who was also the first to exploit a lattice-Boltzmann (LB) technique to this purpose. Of course, LES and LB do not necessarily go along, LB being just an attractive solution technique perfectly suited for parallel computing. Since, in the wake of this pioneering Eggels' paper, the topics of LES and LB have become leading themes in the research group of the present author, this review contains many references to work of Derksen *et al.* (from 1996 onwards) and to many PhD theses and associated papers from this group. Gradually, however, LES (in a Finite Volume, FV, context) is also receiving attention from other research groups and from the commercial software vendors.

II. Various types of fluid flow simulations

Computational fluid dynamics techniques are not capable of fully resolving the highly turbulent flow in most industrial applications within a reasonable time span. In a DNS, all scales of the motion are simulated by means of the classical *Navier–Stokes* (NS) equations. For simulating turbulent flows, this would require that the spacing of the computational grid be sufficiently fine to even resolve the smallest eddies the name of *Kolmogorov* is associated with. As the *Kolmogorov* length scale, η_K, is as small as $\mathrm{Re}^{-3/4}$ times some macroscopic dimension (see, e.g., Tennekes and Lumley, 1972), a 3-D DNS scales with $\mathrm{Re}^{9/4}$ (e.g., Wilcox, 1993; Moin and Kim, 1997). This really limits the applicability of DNS to rather low Reynolds numbers.

Even nowadays, a DNS of the turbulent flow in, e.g., a lab-scale stirred vessel at a low Reynolds number ($\mathrm{Re} = 8{,}000$) still takes approximately 3 months on 8 processors and more than 17 GB of memory (Sommerfeld and Decker, 2004). Hence, the turbulent flows in such applications are usually simulated with the help of the *Reynolds* Averaged *Navier–Stokes* (RANS) equations (see, e.g., Tennekes and Lumley, 1972) which deliver an *averaged* representation of the flow only. This may lead, however, to poor results as to small-scale phenomena, since many of the latter are nonlinearly dependent on the flow field (Rielly and Marquis, 2001).

The exponential increase in computational power along with a drastic drop in price for computer hardware has led to the ability to solve industrial flows by means of LES. The major advantage of LES is that closure is applied to just the

fluctuations that are smaller than the grid spacing, whereas the large turbulent scales are solved explicitly. This means that grid spacing also acts as a low pass filter: fluctuations smaller than the grid spacing are filtered out, i.e., not resolved in the simulation.

It is then assumed that due to this separation in scales, the so-called subgrid scale (SGS) modeling is largely geometry independent because of the universal behavior of turbulence at the small scales. The SGS eddies are therefore more close to the ideal concept of isotropy (according to which the intensity of the fluctuations and their length scale are independent of direction) and, hence, are more susceptible to the application of *Boussinesq*'s concept of turbulent viscosity (see page 163).

Large eddy simulations ask for a fine grid to realize the above separation in scales. LES are therefore computationally more expensive than RANS-based simulations. It is not an option to take refuge to coarse grids in order to reduce simulation times, as LES on a coarse grid does not make sense physically. The grid spacing should be such that at least (a substantial) part of the inertial subrange can be resolved.

Large eddy simulations yield much more detailed simulation results indeed, not only because the grids used easily comprise millions of grid cells—these numbers being larger than common in RANS simulations by at least one order of magnitude—but also because the simulations are inherently transient and reproduce the dynamics of a large proportion of the wide spectrum of eddies. In fact, LES are positioned somewhere in between DNS and RANS. Derksen (2003) carried out LES on a grid of 1.4×10^7 nodes while a DNS would have required a grid of as many as 10^{12} nodes, the latter number being far beyond computational capabilities both currently and in the foreseeable future.

We will now treat the various CFD options in some more detail.

A. Direct Numerical Simulations

The term 'direct' in 'Direct Numerical Simulations' indicates that the flow is fully resolved by solving, without any modeling, the classical NS equations

$$\frac{\partial \mathbf{v}}{\partial t} + \mathbf{v} \cdot \nabla \mathbf{v} = -\frac{1}{\rho} \nabla p + \nu \nabla^2 \mathbf{v} \tag{1}$$

and that not any motion or eddy at whatever scale is ignored, provided that the calculation grid is sufficiently fine. The latter condition implies that refining the grid would (hardly) change the flow field resulting from the simulation. As a matter of fact, laminar flows belong to the type of flows excellently viable to DNS.

Other important targets for DNS are the turbulent flows at Reynolds numbers up to say 10,000 in simple geometries (such as straight channels or curved

pipes), the local flow field around a single particle, or the turbulent two-phase flow in a periodic box of limited size, again under the *proviso* that the calculation grid is sufficiently fine to capture all details of the flow at the scale of particle or box.

B. Large Eddy Simulations

In LES, it is accepted that the flow is not fully resolved: turbulent eddies smaller than the grid spacing Δ are not solved explicitly. These small eddies do contribute, however, to the redistribution of momentum within the flow field. The resulting set of NS equations then runs as

$$\frac{\partial \tilde{\mathbf{v}}}{\partial t} + \tilde{\mathbf{v}} \cdot \nabla \tilde{\mathbf{v}} = -\frac{1}{\rho} \nabla \tilde{p} + v \nabla^2 \tilde{\mathbf{v}} - \nabla \cdot \boldsymbol{\tau} \tag{2}$$

where $\tilde{\mathbf{v}}$ and $\tilde{p}$ now denote the variables to be resolved in the simulation. Note that the latter term in this set of equations represents the effect of SGS stresses that are not calculated explicitly. After having introduced the decomposition

$$\boldsymbol{\tau} = \boldsymbol{\tau}' + \frac{1}{3} tr(\boldsymbol{\tau}) \mathbf{I} \tag{3}$$

the first term at the right-hand side of Eq. (3) is modeled with the help of an effective SGS viscosity coefficient v_e:

$$\boldsymbol{\tau}' = -v_e \left(\nabla \tilde{\mathbf{v}} + (\nabla \tilde{\mathbf{v}})^T \right) \tag{4}$$

while the second term at the right-hand side of Eq. (3) is incorporated into the pressure term of Eq. (2).

This implies that all eddies larger than the grid size are explicitly resolved in a LES. A flow field obtained by means of LES therefore is inherently transient and 3-D. To take advantage of the concept of LES, which is particularly aimed at resolving a great deal of the time and length scales of a turbulent-flow field, fine grids should be used. This implies that LES applied to a flow domain of some size are computationally quite demanding. Restricting LES to 2-D in view of saving computational time does not make sense physically, as the dynamics of turbulent flows in process equipment is inherently 3-D.

In dealing with the SGS terms, Revstedt *et al.* (1998, 2000) and Revstedt and Fuchs (2002) did not use any model; rather, they assumed these terms were just as small as the truncation errors in the numerical computations. This heuristic approach lacks physics and does not deserve copying. A most welcome aspect of LES is that the SGS stresses may be conceived as being isotropic, i.e., insensitive to effects of the larger scales, to the way the turbulence is induced and to the complex and varying boundary conditions of the flow domain. Exactly this

feature renders modeling attractive, in contrast with modeling all turbulent stresses as done in RANS-based simulations (see the next section).

The most widely used model for the SGS stresses is due to Smagorinsky (1963) and involves a SGS eddy viscosity, ν_e, which is related to the local resolved deformation rate $\tilde{S}$:

$$\nu_e = c_s^2 \Delta^2 \sqrt{\tilde{S}^2} \tag{5}$$

with

$$\tilde{S}^2 = \frac{1}{2}\left(\nabla\tilde{\mathbf{v}} + (\nabla\tilde{\mathbf{v}})^T\right) : \left(\nabla\tilde{\mathbf{v}} + (\nabla\tilde{\mathbf{v}})^T\right) \tag{6}$$

While the theoretical value (based on homogeneous, isotropic turbulence) of the Smagorinsky coefficient c_s amounts to 0.165 (Mason and Callen, 1986), in many simulation studies lower values for c_s proved to result in a better reproduction of experimental data. This may have to do with the abundant presence of shear flows in process equipment. Derksen (2003) reported that varying c_s values in the range 0.08–0.14 does not have a large impact on the simulation results. A value of 0.12 is recommended.

At the basis of the *Smagorinsky* SGS model is the assumption of equilibrium between production and dissipation of turbulent kinetic energy in the inertial subrange of eddy sizes. In stirred tanks, however, there is hardly any position where this equilibrium prevails. Furthermore, there is not a good reason why the *Smagorinsky* coefficient should be constant across the flow domain. Other more specific SGS models have therefore been proposed and also investigated as to their impact on the resulting flow fields and turbulence characteristics. Hartmann *et al.* (2004a) assessed the usability of an SGS model due to Voke (more geared to low-Reynolds number turbulence), while Derksen (2001) investigated a so-called structure function SGS model for a turbulent viscosity that depends on eddy size. Derksen (2006a) supplemented the standard *Smagorinsky* SGS model with wall-damping functions to bring the eddy viscosity explicitly to zero at solid walls, since in physical reality velocity fluctuations and subgrid stresses are zero at walls. Recently, *FLUENT 6.2* came with several new SGS models. Further refinements in SGS modeling may be expected to improve the accuracy of LES.

An inherent property of the LES approach is that the simulated flow field is no longer steady, but exhibits a transient character due to the presence and motion of large-scale eddies. The LES methodology has proven to be a powerful tool for studying and visualizing stirred tank flows (Eggels, 1996; Derksen *et al.* 1999; Bakker *et al.*, 2000; Derksen, 2001; Bakker and Oshinowo, 2004), as it inherently takes the unsteady and periodic behavior of the flow (around impeller and baffles) into account.

C. Reynolds Averaged Navier–Stokes Simulations

The focus of RANS simulations is on the time-averaged flow behavior of turbulent flows. Yet, all turbulent eddies do contribute to redistributing momentum within the flow domain and by doing so make up the inherently transient character of a turbulent-flow field. In RANS, these effects of the full range of eddies are made visible via the so-called *Reynolds* decomposition of the NS equations (see, e.g., Tennekes and Lumley, 1972, or Rodi, 1984) of the flow variables into mean and fluctuating components. To this end, a clear distinction is required between the temporal and spatial scales of the mean flow on the one hand and those associated with the turbulent fluctuations on the other hand.

Via this *Reynolds* decomposition and after subsequent averaging all terms of the NS equations, the so-called turbulent or *Reynolds* stresses $\overline{u_i u_j}$ emerge in the transport equations, where these stresses represent the additional averaged momentum transport due to the eddies. These stresses may be resolved explicitly from separate transport equations which in suffix notation (usual in the field of turbulence) look as follows:

$$\frac{\partial \overline{u_i u_j}}{\partial t} + u_k \frac{\partial \overline{u_i u_j}}{\partial x_k} = P_{ij} + D_{ij} - \varepsilon_{ij} + \Pi_{ij} \tag{7}$$

in which the first three terms of the right-term side denote the production, diffusion, and dissipation of the turbulent stresses, respectively, while the last term is the so-called pressure-strain term that represents the redistribution of the turbulent kinetic energy among the three coordinate directions that makes the turbulence more isotropic (Rodi, 1984). Several of these terms need modeling for which a gamut of choices is available. In principle, this approach implies the need of solving nine more partial differential equations per grid cell. As a result, CPU times required for computational simulations on the basis of some *Reynolds* Stress Model (RSM) are relatively high.

A cure against these longer CPU times is the Algebraic Stress Model (ASM) described by, e.g., Rodi (1984) and used and recommended by, e.g., Bakker (1992) and Bakker (1996). Most commercial codes do no longer support an ASM.

Usually, however, the stresses are modeled with the help of a single turbulent viscosity coefficient that presumes isotropic turbulent transport. In the RANS-approach, a turbulent or eddy viscosity coefficient, ν_t, covers the momentum transport by the *full* spectrum of turbulent scales (eddies). Frisch (1995) recollects that as early as 1870 Boussinesq stressed turbulence greatly increases viscosity and proposed an expression for the eddy viscosity. The eventual set of equations runs as

$$\frac{\partial \mathbf{V}}{\partial t} + \mathbf{V} \cdot \nabla \mathbf{V} = -\frac{1}{\rho} \nabla P + (\nu + \nu_t) \nabla^2 \mathbf{V} \tag{8}$$

In its turn, the turbulent viscosity may be position dependent and generally may be modeled in terms of a model, very usually a k–ε model:

$$\nu_t = C_\mu \frac{k^2}{\varepsilon} \tag{9}$$

where k is the concentration of turbulent kinetic energy in J/kg (or m^2/s^2) and ε is the rate of dissipation (in W/kg, or $m^2/s^2/s$) of this turbulent kinetic energy. These two concentrations k and ε are generally conceived as the most important parameters describing a turbulent-flow field. In their turn, their spatial distributions within the turbulent-flow domain may be calculated from the following transport equations for k and ε, respectively:

$$\frac{\partial k}{\partial t} + u_i \frac{\partial k}{\partial x_i} = P_k + D_k - \varepsilon + \Pi_k \tag{10}$$

the right-hand side of which contains similar terms as the above transport equations for the turbulent stresses, and

$$\frac{\partial \varepsilon}{\partial t} + u_i \frac{\partial \varepsilon}{\partial x_i} = P_\varepsilon + D_\varepsilon - \Omega \tag{11}$$

in which the last term denotes the destruction of ε. The interested reader is referred to, e.g., Rodi (1984) for the meaning of all these right-hand terms and their modeling. The assumption often used in classical turbulence theory that production and dissipation of turbulent kinetic energy balance *locally*, is found by putting in Eq. (10) all terms but the first and third at the right-hand side equal to zero.

These two transport equations for k and ε form an inherent part of any k–ε model of RANS-simulations. As the result of 'closing' the turbulence modeling such that no further unknown variables and equations are introduced, the ε-equation does contain some terms that are still the result of modeling, albeit at the very small scales (e.g., Rodi, 1984).

The (isotropic) eddy viscosity concept and the use of a k–ε model are known to be inappropriate in rotating and/or strongly 3-D flows (see, e.g., Wilcox, 1993). This issue will be addressed in more detail in Section IV. Some researchers prefer different models for the eddy viscosity, such as the k–ω model (where ω denotes vorticity) that performs better in regions closer to walls. For this latter reason, the k–ε model and the k–ω model are often blended into the so-called Shear-Stress-Transport (SST) model (Menter, 1994) with the view of using these two models in those regions of the flow domain where they perform best. In spite of these objections, however, RANS simulations mostly exploit the eddy viscosity concept rather than the more delicate and time-consuming RSM turbulence model. They deliver simulation results of—in many cases—reasonable or sufficient accuracy in a cost-effective way.

RANS-based simulations exploiting the eddy viscosity concept just reproduce the average flow field and the spatial distribution of turbulence properties such as k and ε. As such, RANS-based simulations are excellently suited for identifying dead zones, recirculatory flows, short-circuiting between entrance and exit, and further undesired flow features. Even in transient RANS-based simulations, however, it is not a priori clear which part of the fluctuations is temporally resolved and which part is taken care of by the turbulence model. This inherent property of RANS-based simulations especially raises concerns in the case of flows exhibiting no clear spectral separation between low-frequency coherent motions (such as macroinstabilities, precessing vortices, and trailing vortices) and turbulent fluctuations (making part of the cascade of eddies or whirls typical of turbulence); and: ''A mechanistic picture of turbulence cannot be treated on the average since such flows are dynamic.'' (Praturi and Brodkey, 1978).

Yet (steady) RANS-based simulations are attractive as they relatively cheaply deliver a quick impression of the overall flow field in the vessel. Effects on the overall flow field of varying the position of impeller, feed pipe, withdrawal pipe, and/or heat coil can easily be explored.

Note that the Eqs. (1), (2), and (8) are really and essentially different due to the absence or presence of different turbulent transport terms. Only by incorporating dedicated formulations for the SGS eddy viscosity can one attain that LES yield the same flow field as DNS. RANS-based simulations with their turbulent viscosity coefficient, however, essentially deliver steady flow fields and as such are never capable of delivering the same velocity fields as the inherently transient LES or DNS, irrespectively of the refinement of the computational grid!

D. The Simulation of Processes in a Turbulent Single-Phase Flow

For simulating computationally the spatial and temporal evolution of both physical and chemical processes in mixing devices operated in a turbulent single-phase mode, two essentially different approaches are available: the Lagrangian approach and the Eulerian technique. These will be explained briefly.

In the Lagrangian approach, individual parcels or blobs of (miscible) fluid added via some feed pipe or otherwise are tracked, while they may exhibit properties (density, viscosity, concentrations, color, temperature, but also vorticity) that distinguish them from the ambient fluid. Their path through the turbulent-flow field in response to the local advection and further local forces (*if applicable*) is calculated by means of Newton's law, usually under the assumption of 'one-way coupling' that these parcels do not affect the flow field. On their way through the tank, these parcels or blobs may mix or exchange mass and/or temperature with the ambient fluid or may adapt shape or internal velocity distributions in response to events in the surrounding fluid.

In real life, the parcels or blobs are also subjected to the turbulent fluctuations not resolved in the simulation. Depending on the type of simulation (DNS, LES, or RANS), the wide range of eddies of the turbulent-fluid-flow field is not necessarily calculated completely. Parcels released in a LES flow field feel both the resolved part of the fluid motion and the unresolved SGS part that, at best, is known in statistical terms only. It is desirable that the forces exerted by the fluid flow on the particles are dominated by the known, resolved part of the flow field. This issue is discussed in greater detail in the next section in the context of tracking real particles. With a RANS simulation, the turbulent velocity fluctuations remaining unresolved completely, the effect of the turbulence on the tracks is to be mimicked by some stochastic model. As a result, particle tracking in a RANS context produces less realistic results than in an LES-based flow field.

An early example of tracking fluid parcels in a stirred tank can be found in Bouwmans (1992) and Bouwmans *et al.* (1997). Bakker (1996) used a tracking routine with the view to provide a Lagrangian description of micromixing in a stirred tank chemical reactor. Lapin *et al.* (2004) recently described a computational strategy for 'travelling along the lifelines' of single cells (i.e., tracking them) in stirred bioreactors in order to characterize the dynamics of the heterogeneous cell population and to study the impact of spatial and dynamic variations in concentrations of substrates and products across the reactor.

The motions of the individual fluid parcels may be overlooked in favor of a more global, or Eulerian, description. In the case of single-phase systems, convective transport equations for scalar quantities are widely used for calculating the spatial distributions in species concentrations and/or temperature. Chemical reactions may be taken into account in these scalar transport equations by means of source or sink terms comprising chemical rate expressions. The pertinent transport equations run as

$$\frac{\partial T}{\partial t} + \mathbf{v} \cdot \nabla T = \kappa \nabla^2 T + q \tag{12}$$

and

$$\frac{\partial c}{\partial t} + \mathbf{v} \cdot \nabla c = D \nabla^2 c + r \tag{13}$$

In Eq. (13), r stands for the production (or consumption) of the species of interest due to a chemical reaction, while in Eq. (12) q represents the heat production, e.g., due to one of more chemical reactions. Equation (13) is often referred to as the *Convection-Diffusion-Reaction* (CDR) equation.

Since turbulent fluctuations not only occur in the velocity (and pressure) field but also in species concentrations and temperature, the convection diffusion equations for heat and species transport under turbulent-flow conditions also comprise cross-correlation terms, obtained by properly averaging products of

velocity–concentration, velocity–temperature, concentration–temperature, and concentration–concentration fluctuations, on the analogy of the *Reynolds* stresses in the NS equations (e.g., Patterson, 1985; Ranade, 2002). The challenge is still to find appropriate closure relations for these cross-correlation terms: these may be either phenomenological or mechanistic ('micromixing models') or probabilistic (exploiting probability density functions, PDFs).

In stirred chemical reactors, unlike in combustion and with other gas-phase reactions, these closure terms should take into account that for liquids the Schmidt number ($Sc = \nu/D$) is in the order 100–1,000, and, hence, the role of species diffusion at scales within the *Kolmogorov* eddies should explicitly be taken into account (Kresta and Brodkey, 2004). Essential is that diffusion of chemical species is governed by the *Batchelor* length scale η_B which obeys to

$$\eta_B = \eta_K Sc^{-1/2} \tag{14}$$

which for large *Sc* numbers is much smaller than the *Kolmogorov* length scale η_K indeed. Such so-called micromixing processes have to be described by means of micromixing models which will be dealt with in some greater detail in Section VIII.

These convective transport equations for heat and species have a similar structure as the NS equations and therefore can easily be solved by the same solver simultaneously with the velocity field. As a matter of fact, they are much simpler to solve than the NS equations since they are linear and do not involve the solution of a pressure term via the continuity equation. In addition, the usual assumption is that spatial or temporal variations in species concentration and temperature do not affect the turbulent-flow field (another example of one-way coupling).

E. The Computational Fluid Dynamics of Two-Phase Flows

On the analogy of simulating the process of adding blobs of a miscible liquid, two-phase flow in stirred tanks in a RANS context may be treated in two ways: Euler–Lagrange or Euler–Euler, with the second, dispersed phase treated according to a Lagrangian approach and from a Eulerian point of view, respectively.

1. Euler–Lagrangian Approach

The Euler–Lagrangian approach is very common in the field of dilute dispersed two-phase flow. Already in the mid 1980s, a particle tracking routine was available in the commercial CFD-code *FLUENT*. In the Euler–Lagrangian approach, the dispersed phase is conceived as a collection of individual particles (solid particles, droplets, bubbles) for which the equations of motion can be solved individually. The particles are conceived as *point particles* which move

across the flow domain in response to the turbulent-flow field of the carrier phase. The consequence of treating particles as *point particles* is that the detailed flow between the particles in response to the presence and motion of the particles is not resolved.

For the hydrodynamics forces acting on the particles, mostly single-particle expressions are used; this implies that hydrodynamic interactions between particles are ignored completely. In many cases, direct interactions of particles owing to collisions are ignored as well. All this—along with the computational burden that increases linearly with the number of particles being tracked—may limit the practical applicability of the method to dilute systems with relatively low volume fractions of dispersed phase and/or to flow domains of small size. By feeding back the reactive forces exerted by the particles on the continuous carrier phase, two-way coupling between the two phases is obtained.

Without much discussion, one may anticipate that particle inertia, gravity, and drag force need to be part of the equations of motion describing the motion and paths of the particles. Since a stirred tank is very inhomogeneous and exhibits strong gradients in velocity, pressure, and stress fields, it is difficult to estimate a priori if more exotic fluid-particle forces such as the *Saffman* lift force, the *Magnus* force, and the *history* force may play a role of significance either globally or locally. For a concise summary about these forces and for expressions for these forces, the reader is referred to, e.g., Derksen (2003). Added mass may be important for bubbly flows. It is obvious that in such a Lagrangian approach distributions in particle size may easily be taken into account.

As discussed earlier in the context of tracking miscible parcels or blobs, particles travel through the resolved average or fluctuating velocity field as well as feel the unresolved velocity fluctuations. Since the major fluid-particle force may be the drag force, the fluid's velocity field is of primary importance, the turbulent velocity fluctuations inclusively, whether or not they are resolved in the simulation; fluctuations in pressure and stresses may be secondary. Supplying stochastic variations on top of the resolved velocity field mimics the unresolved fluctuations and brings the expected seemingly erratic paths of the particles about.

Of course, the role of the artificially introduced stochastics for mimicking the effect of all eddies in a RANS-based particle tracking is much more pronounced than that for mimicking the effect of just the SGS eddies in a LES-based tracking procedure. In addition, the random variations may suffer from lacking the spatial or temporal correlations the turbulent fluctuations exhibit in real life. In RANS-based simulations, these correlations are not contained in the steady spatial distributions of k and ε and (*if applicable*) the *Reynolds* stresses from which a typical turbulent time scale such as k/ε may be derived. One may try and cure the problem of missing the temporal coherence in the velocity fluctuations by picking a new random value for the fluid's velocity only after a certain period of time has lapsed.

In LES-based simulations, just the SGS part of the turbulence spectrum needs to be mimicked by stochastics. The idea is that the resolved eddies have the biggest impact on the paths of the particles indeed. This requires not only that the resolved velocity fluctuations should be stronger than the (estimated) SGS fluctuations, but also that the particle relaxation time should be larger than the time-step applied in the LES. Meeting the latter criterion implies that the time step of the LES is capable of keeping up with the time scale the particle needs to respond to changes in the flow field of the surrounding fluid. In the context of LES, picking a new random velocity only after (part of) a time k_{sgs}/ε has lapsed may cure the problem of missing the coherence in the SGS eddies when mimicking the effect of the SGS eddies on the particle tracks. Here, k_{sgs} stands for the kinetic energy associated with the SGS eddies only and has to be estimated. All these issues have been extensively discussed by, e.g., Derksen (2003, 2006a).

2. *Euler–Euler Approach*

In the complete Eulerian description of multiphase flows, the dispersed phase may well be conceived as a second continuous phase that interpenetrates the real continuous phase, the carrier phase; this approach is often referred to as *two-fluid formulation*. The resulting 'simultaneous' presence of two continua is taken into account by their respective volume fractions. All other variables such as velocities need to be averaged, in some way, in proportion to their presence; various techniques have been proposed to that purpose leading, however, to different formulations of the continuum equations. The method of ensemble averaging (based on a statistical average of individual realizations) is now generally accepted as most appropriate.

In the two-fluid formulation, the motion or velocity field of each of the two continuous phases is described by its own momentum balances or NS equations (see, e.g., Rietema and Van den Akker, 1983 or Van den Akker, 1986). In both momentum balances, a phase interaction force between the two continuous phases occurs predominantly, of course with opposite sign. Two-fluid models therefore belong to the class of two-way coupling approaches. The continuum formulation of the phase interaction force should reflect the same effects as experienced by the individual particles and discussed above in the context of the Lagrangian description of dispersed two-phase flow.

One therefore has to decide here which components of the phase interaction force (drag, virtual mass, *Saffman* lift, *Magnus*, history, stress gradients) are relevant and should be incorporated in the two sets of NS equations. The reader is referred to more specific literature, such as Oey *et al*. (2003), for reports on the effects of ignoring certain components of the interaction force in the two-fluid approach. The question how to model in the two-fluid formulation (lateral) dispersion of bubbles, drops, and particles in swarms is relevant

as well: various models are available. See also the discussion on page 204 as to (Eq. (19)).

Another important issue in two-fluid models is about modeling the turbulent stresses under two-phase conditions (e.g., Van den Akker, 1998). At this moment, there is still no consensus on a universal two-phase turbulence model. Generally, turbulence in the continuous phase may be generated by shear due to large-scale velocity gradients felt by the continuous phase itself (just like in single-phase flows) as well as by the presence and relative motion of the dispersed phase particles. The ratio at which these two mechanisms contribute to the generation of turbulence may be an important factor in drafting a universal model. In addition, the dispersed phase may exhibit a turbulent-flow behavior in response to the turbulent motions of the continuous phase in which it is embedded; this response may depend on several time scales and their interaction (Oey *et al.*, 2003). Lance *et al.* (1991) suggested that the motion of bubbles promotes a return to isotropy (see also Van den Akker, 1998). A universal model, however, is not available right now.

In dense systems such as encountered in solids suspension, particle–particle interaction may be important as well. Then, the closure of solid-phase stresses is an important issue for which kinetic theory models and solids phase viscosity may be instrumental (see, e.g., Curtis and Van Wachem, 2004).

As a matter of fact, in comparison with the Euler–Lagrangian approach, the complete Eulerian (or Euler–Euler) approach may better comply with denser two-phase flows, i.e., with higher volume fractions of the dispersed phase, when tracking individual particles is no longer doable in view of the computational times involved and the computer memory required, and when the physical interactions become too dominating to be ignored. Under these circumstances, the motion of individual particles may be overlooked and it is wiser to opt for a more superficial strategy that, however, still has to take the proper physics into account.

Precisely owing to the continuum description of the dispersed phase, in Euler–Euler models, particle size is *not* an issue in relation to selecting grid cell size. Particle size only occurs in the constitutive relations used for modeling the phase interaction force and the dispersed-phase turbulent stresses.

In the case of droplets and bubbles, particle size and number density may respond to variations in shear or energy dissipation rate. Such variations are abundantly present in turbulent-stirred vessels. In fact, the explicit role of the revolving impeller is to produce small bubbles or drops, while in substantial parts of the vessel bubble or drop size may increase again due to locally lower turbulence levels. Particle size distributions and their spatial variations are therefore commonplace and unavoidable in industrial mixing equipment. This seriously limits the applicability of common Euler–Euler models exploiting just a single value for particle size. A way out is to adopt a multifluid or multiphase approach in which various particle size classes are distinguished, with mutual transition paths due to particle break-up and coalescence. Such models will be discussed further on.

III. Computational Aspects

As the continuity equation, the NS equations, and the transport equations for the turbulent variables are highly nonlinear, any CFD-calculation is essentially iterative. Generally, the convergence rate of simulations depends on the number of grid points and on the number of equations to be solved.

The number of grid points is associated with the desired or required degree of detail and accuracy of the simulations given the type of simulation selected. In running a DNS (provided it is doable) one is interested in a fully resolved flow field and the grid should be sufficiently fine to catch all motions. In running a LES, the grid should be sufficiently fine for the subgrid scales to become independent of the macroflow.

The number of equations to be solved is, among other things, related to the turbulence model chosen (in comparison with the k–ε model, the RSM involves five more differential equations). The number of equations further depends on the character of the simulation: whether it is 3-D, $2^{1/2}$-D, or just 2-D (see below, under 'The domain and the grid'). In the case of two-phase flow simulations, the use of two-fluid models implies doubling the number of NS equations required for single-phase flow. All this may urge the development of more efficient solution algorithms. Recent developments in computer hardware (faster processors, parallel platforms) make this possible indeed.

Various numerical techniques are available for discretizing the set of partial differential equations to be solved. Discretizing essentially is the method of converting the (partial) differential into algebraic equations by transforming (partial) derivatives into finite-difference formulations. First of all, most (commercial) flow simulation codes exploit the finite-volume (or finite-difference) method that has been discussed extensively by Shyy (1994). An introduction to the concept can be found with, e.g., Abbott and Basco (1989) and Shaw (1992). Many more techniques are available for discretization, such as finite-element, spectral, arc-length, and filter-scheme methods, which are beyond the scope of the present review. The result is a (large) set of algebraic equations anyway: one algebraic equation per grid point for each flow variable that connects the value of a particular flow variable at a particular grid point with those at a number of neighboring grid points.

A. Finite Volume Techniques

Most commercial CFD-codes are based upon the ideas and numerical methods developed back in the 1970s at Imperial College London by Spalding, Patankar, Gosman, and others:

- the FV formulation (the natural balance formulation of the NS equations and the continuity equation),

- the staggered grid concept (velocity components and scalar quantities such as pressure are not defined at the same mesh points),
- the common discretization schemes (central, upwind, quadratic upwind),
- the pressure–velocity coupling according to the Semi-Implicit Method for Pressure Linked Equations (SIMPLE) or related algorithms, and
- the matrix solvers for the resulting sets of algebraic equations.

Useful reviews of these basic elements of CFD can be found with Patankar (1980), Abbott and Basco (1989), Shaw (1992), and Ranade (2002). In the meantime, substantial progress has been realized in developing more effective and powerful numerical techniques. Several of them have made it into the common commercial CFD packages. Just as an example, several of the commercial vendors have incorporated the option of collocated grids. A few more important issues should be highlighted here.

First of all, the current iterative solution procedures solve the various momentum equations successively; although this highly segregated solution technique does not require large computer memory capacity, it does result in slow convergence and, hence, in long CPU times. Reducing the degree of separation, i.e., coupling several momentum equations and solving them simultaneously, substantially speeds up the convergence rate of the calculation and reduces the number of iterations required (Van Santen *et al.*, 1996); the larger matrices do make greater demands on computer memory.

Second, the various discretization schemes common to all commercial software may suffer from the appearance of spurious oscillations (wiggles) in regions of strong gradients and from numerical or false diffusion, or smearing (Shyy, 1994). Finding the optimum scheme to avoid numerical diffusion is often not very easy, especially in convection-dominated flows, when direction of flow and grid orientation do not match everywhere. Wiggles may pose a serious problem in solving turbulent flows, multiphase flows, and species transport as the pertinent equations contain variables that are inherently positive, such as k, ε, phase fractions and concentrations. For these variables, wiggles may not be tolerated as they could give rise to negative values which may result in divergence of the algorithm. Although adaptive grid techniques, e.g., local grid refinement, may cure the problem of oscillations, the most promising among the modern schemes seems to be the antidiffusion concept of Total Variation Diminishing (TVD) that has proliferated in quite a few variants. By adding subgrid points, TVD schemes do increase the calculational burden. In *FLUENT 6.2*, a bounded central differencing scheme is switched on for LES, replacing the second-order upwind scheme which by default discretizes the convective terms in RANS-based simulations.

Third, writing the discretized equations in matrix form results in sparse matrices, often of a tri-diagonal form, which traditionally are solved by successive under- or over-relaxation methods using the tri-diagonal matrix algorithm

(TDMA). In the 1990s, however, two novel classes of methods have entered the scene, viz.

- Krylov subspace methods (such as Conjugate Gradient CG, the improved BiCGSTAB, and GMRES) in combination with preconditioners for matrix manipulations aimed at enhanced convergence, and
- Multigrid methods in which convergence is improved by solving the equations in, e.g., a nested iteration on multiple grids, starting, e.g., on a coarse grid and then moving to a finer grid, *et cetera*.

For a more detailed description of these more sophisticated solution methods the reader is referred to, e.g., Vuik (1993) and Shyy (1994). Adopting these more sophisticated solution techniques becomes more important with increasing number of partial differential equations to be solved, such as in two-phase flow CFD (see, e.g., Lathouwers and Van den Akker, 1996; Van Santen *et al*., 1996; Lathouwers, 1999).

In the last decade, most new algorithms, schemes, solvers, and preconditioners have found their way into most commercial software packages. Multigrid solvers are also available. Furthermore, all CFD vendors have developed powerful pre- and post processing routines.

B. The Size of the Computations

The number of grid points used for CFD-studies of stirred tanks strongly varies with the type of CFD and generally increases in time. While for Bakker and Van den Akker (1994a, b) the maximum number of grid points amounted to some 25,000, these days hundreds of thousands grid points are not uncommon for RANS-simulations. Usually, DNS and LES are carried out with the view to arrive at very fine spatial and temporal resolutions; then, substantially more grid points are needed than with RANS-based simulations. For his LES, Eggels (1996) used two uniform grids comprising 1.73×10^6 and 13.8×10^6 nodes, respectively. Derksen and Van den Akker (1999) used up to 6×10^6 grid points, Hollander *et al*. (2000) some 2×10^6, Derksen (2001), Lu *et al*. (2002), and Hartmann *et al*. (2006) up to some 13.8×10^6, while Ten Cate *et al*. (2000) went as high as 35×10^6 grid points for an industrial crystallizer.

In addition, adding more transport equations for simulating physical or chemical processes and running CFD for multiphase flows increases the size of the computational jobs, both in the number of equations to be solved and in terms of the difficulty of getting the solution converged.

Advanced CFD simulations (both in terms of numbers of grid points and partial differential equations) therefore require increasing amounts of computer memory and CPU-time. Chemical engineers increasingly get familiar with the idea of exploiting CFD, though still mostly of the RANS-type. Gradually, the

advantages of LES become more obvious. These days, it becomes attractive to speed up CFD simulations by running them on parallel computer platforms: a cluster of pc's operating under, e.g., LINUX, or a massive parallel machine (e.g., a CRAY). In this way, larger CFD simulations can be run overnight or over the weekend. In addition, computer hardware (processors, memory) keep becoming faster and cheaper. Just to illustrate what currently is becoming feasible: Derksen (2006a) carried out his LES job on a platform of 12 CPU's, and needed 7 h of wall-clock time for a single impeller revolution; as a mater of fact, such a simulation yields an incredible degree of detail.

Parallel computing requires software made suitable for operating on parallel processors. Decomposition of the flow domain and attributing each domain to a separate processor is the common procedure. A fast communication between the various processors is crucial, not to partly spoil the gain obtained by going parallel.

Although commercial CFD vendors make versions of their software suited for parallel computing, it is precisely the promises of parallel computing that turn the Lattice Boltzmann techniques into an attractive option. The locality of the collision operation in this technique (see below) along with a high computational efficiency allows for simulating complex flow systems with high spatial and temporal resolution. Furthermore, the efficiency of the scheme hardly depends on the complexity of the flow domain. Compared to the conventional FV solvers of the current commercial CFD codes, which should be robust and suited for a wide variety of flow problems and flow conditions, a LB solver is faster by at least one order of magnitude (see, e.g., Table I). All these properties make LB very attractive for LES in complex geometries and even very competitive in comparison with the conventional FV techniques.

TABLE I

NUMERICAL SETTINGS OF TWO SIMULATIONS ON A GAS CYCLONE WITH DIFFERENT NUMERICAL SCHEMES: A RANS-BASED SIMULATION (HOEKSTRA, 2000) AND A LES DUE TO DERKSEN AND VAN DEN AKKER (2000)

	RANS	LES
Numerical scheme	Finite volume (FLUENT)	Lattice-Boltzmann
Spatial and temporal properties	3-D, steady state	3-D, transient
Number of grid nodes	1.2×10^5	4.9×10^6
Total wall-clock time per simulation[a]	117 h[b]	864 h[c]
Wall-clock time per grid node per step[d]	1.7×10^{-4} s	6.1×10^{-6} s

Both simulations were run on an HP Convex S-Class computer.

[a]Based on a simulation on one processor.

[b]Converged after 20,000 iterations.

[c]Required 95,500 time steps for obtaining reliable flow field statistics.

[d]One 'step' denotes one 'time step' or one 'iteration step.'

C. Lattice-Boltzmann Techniques

Very promising with a view to simulating turbulent flows is the LB scheme. The method originates from lattice-gas automata, which for fluid flow applications were introduced by Frisch *et al.* (1986) and by McNamara and Zanetti (1988) and has been studied, refined, and applied ever since. In spite of LB being relatively new and still 'under construction,' the method receives an increasing amount of attention among scientists and engineers. Rather than taking the discretized NS equations as a starting point for the numerical analysis, a discrete system that mimics fluid flow is designed directly.

Although LB therefore nowadays may be considered as a solver for the NS equations, there is definitely more behind it. The method originally stems from the *lattice gas automaton* (LGA), which is a *cellular automaton*. In a LGA, a fluid can be considered as a collection of discrete particles having interaction with each other via a set of simple collision rules, thereby taking into account that the number of particles and momentum is conserved.

In the LB technique, the fluid to be simulated consists of a large set of fictitious particles. Essentially, the LB technique boils down to tracking a collection of these fictitious particles residing on a regular lattice. A typical lattice that is commonly used for the effective simulation of the NS equations (Somers, 1993) is a 3-D projection of a 4-D face-centred hypercube. This projected lattice has 18 velocity directions. Every time step, the particles move synchronously along these directions to neighboring lattice sites where they collide. The collisions at the lattice sites have to conserve mass and momentum and obey the so-called collision operator comprising a set of collision rules. The characteristic features of the LB technique are the distribution of particle densities over the various directions, the lattice velocities, and the collision rules.

Such an approach is conceptually different from the continuum description of momentum transport in a fluid in terms of the NS equations. It can be demonstrated, however, that, with a proper choice of the lattice (viz. its symmetry properties), with the collision rules, and with the proper redistribution of particle mass over the (discrete) velocity directions, the NS equations are obeyed at least in the incompressible limit. It is all about translating the above characteristic LB features into the physical concepts momentum, density, and viscosity. The collision rules can be translated into the common variable 'viscosity,' since colliding particles lead to viscous behavior indeed. The reader interested in more details is referred to Succi (2001).

Lattice-Boltzmann is an inherently time-dependent approach. Using LB for steady flows, however, and letting the flow develop in time from some starting condition toward a steady-state is not a very good idea, since the LB time steps need to be small (compared to, e.g., FV time steps) in order to meet the incompressibility constraint.

The LB method is especially attractive if complexly shaped boundaries are involved; see, e.g., Chen and Doolen (1998). Eggels (1996) was the first to study

the flow near a Rushton turbine in a baffled stirred tank reactor by means of a LES, thereby using LB on a uniform grid. Derksen and Van den Akker (1998, 1999) performed a similar study for a tank reactor where the flow was driven by either a pitched blade turbine or a Rushton turbine. These simulations revealed a range of flow field characteristics, such as the turbulence statistics and the trailing vortex structure near the impeller. The computer code they developed is based on a LB scheme proposed by Somers (1993). Boundary conditions can be imposed through locally forcing the fluid to a prescribed velocity, or (in case of no-slip walls) by simple bounce-back rules for the fictitious LB particles. In an agitated vessel, the action of the revolving impeller is described by means of an adaptive force-field procedure (Derksen and Van den Akker, 1998, 1999).

Lattice-Boltzmann can simply be conceived as an alternative method of finding a solution for the NS equations and is now being used for a growing number of applications, ranging from laminar blood flow through irregularly shaped veins (Artoli *et al*., 2003), the swirling flow in a vessel with a revolving bottom (Derksen *et al*., 1996) and the vortex street behind a cylinder in cross-flow (Derksen *et al*., 1997) to turbulent flow in industrial devices such as stirred vessels, swirl tubes and reverse flow cyclones (Derksen and Van den Akker, 1998, 1999, 2000; Derksen, 2001, 2002a, b). There is also a commercial LB code available (*Power FLOW*, EXA Corp., USA) that is used for flow problems related to, e.g., the automotive and aerospace industries.

A disadvantage of LB techniques is that they require a (locally) uniform and cubic computational grid. This raises problems with curved boundaries (see Section III). Furthermore, the flow is calculated in great detail everywhere, irrespective of the degree of turbulence; in some parts of the flow domain, particularly in the more quiescent parts of the vessel, the LES may turn into some type of DNS, the SGS contribution to the transport equation becoming quite obsolete. Rohde (2004) developed a technique for local grid refinement which, however, has not yet been applied to the cylindrical geometry of a stirred vessel. Lu *et al*. (2002) successfully attempted the use of a nonuniform grid in their LB LES of the turbulent flow in a stirred tank.

Eggels and Somers (1995) used an LB scheme for simulating species transport in a cavity flow. Such an LB scheme, however, is more memory intensive than a FV formulation of the convective-diffusion equation, as in the LB discretization typically 18 single-precision concentrations (associated with the 18 velocity directions in the usual lattice) need to be stored, while in the FV just 2 or 3 (double-precision) variables are needed. Scalar species transport therefore can better be simulated with an FV solver.

D. A Mutual Comparison of Finite Volume and Lattice-Boltzmann

Lattice-Boltzmann exhibits some inherent properties that favor the speed of the simulations, and therefore make the method a serious candidate and

alternative for FV techniques for simulating flows in process industry equipment. These properties are:

- The hydrodynamic quantities such as the velocities and velocity gradients are determined *locally* in a LB code. As a result, the local character of the LB technique is strongly in favor of (massive) parallellization of the computational job via domain decomposition: the communication between CPU's relates to grid cells very near to the subdomain boundaries only. On the contrary, in solving the NS equations iteratively with a FV solver the field properties result in long-range variations propagating across the boundaries of subdomains and, hence, requiring intense communication between CPU's dealing with neighboring subdomains.
- Since LB describes the NS equations *in the incompressible limit*, the local pressures can directly be obtained from the local densities and the speed of sound. Hence, a distinct step for calculating the pressures via a Poisson equation (derived from the continuity equation) as required in incompressible FV schemes, is absent in LB.
- Implementing complex boundaries in LB simulations is relatively easy compared to doing so for FV techniques (Chen and Doolen, 1998). In view of the usually complex boundaries of process equipment, particularly in the case of stirred vessels with a revolving impeller, this is a distinctive advantage.
- More basically, LB with its collision rules is intrinsically simpler than most FV schemes, since the LB equation is a fully explicit first-order discretized scheme (though second-order accurate in space and time), while temporal discretization in FV often exploits the Crank–Nicolson or some other mixed (i.e., implicit) scheme (see, e.g., Patankar, 1980) and the numerical accuracy in FV provided by first-order approximations is usually insufficient (Abbott and Basco, 1989). Note that 'fully explicit' means that the value of any variable at a particular moment in time is calculated from the values of variables at the previous moment in time only; this calculation is much simpler than that with any other implicit scheme.

A comprehensive and more extensive overview of the pros and cons of LB with respect to applications can be found in Succi (2001). By the way, LB methods are continuously improved to increase speed and accuracy, particularly by introducing grid refinement techniques and advanced techniques for arbitrarily shaped boundaries (e.g., Rohde *et al.*, 2002, 2003, 2006; Rohde, 2004).

It makes sense to compare the implications (in terms of simulation times) of using FV vs. LB in simulating turbulent-flow fields in process devices. Hoekstra (2000) demonstrated the numerical implications of applying different numerical schemes in an industrial application. He compared the outcome of his RANS simulation for a gas cyclone with that of a LES carried out by Derksen and Van den Akker (2000). Table I presents a number of numerical features of the two types of simulations.

Not only did the results of the LES agree much better with the experimental data than those of the RANS simulation, the LB code was also roughly 30 times faster than the FV code in terms of simulation time per grid node per step. To put it in a more practical sense: performing this LES on, e.g., 18 processors with the FV code would take 2 months, whereas a simulation as such with LB would take 2 days only.

Another comparison is due to Van Wageningen *et al.* (2004) who performed a similar study (in terms of the numerical scheme used) on unsteady laminar flow in a Kenics® static mixer. They found that the LB code was 500–600 times faster than *FLUENT* in terms of simulation time per grid node per time step and that *FLUENT* used about 5 times more memory than LB.

The difference in speed between a LB code and a FV code in the above studies partly originates from their different character: the FV code in a general-purpose commercial CFD code should be robust and suited in many applications, while the LB codes used are of a research type and usually strongly dedicated and geared to a specific job.

IV. Boundary Conditions

Solving sets of (partial) differential equations inherently requires the specification of boundary conditions and, in case of transient simulations, also initial conditions. This is not as simple as it looks like, especially for turbulent flows in complex process equipment.

Whenever a free surface is present at some (mean) fixed position, most CFD codes assume it to be strictly flat, while in the direction normal to the free surface velocities and gradients of most variables are taken zero. Usually, this is accomplished by defining 'mirror cells' at the free surface. It is not clear what the effect is of the use of such mirror cells on the flow field in the upper part of the vessel in comparison with real life where the surface is not necessarily flat.

A. Moving Boundaries

An aspect of CFD in stirred vessels that needs separate discussion is the issue of the revolving impeller and the way its motion is dealt with in the simulations.

In the early days, see, e.g., Bakker and Van den Akker (1994a), a black box representing the impeller swept volume was often used in RANS simulations, with boundary conditions in the outflow of the impeller which were derived from experimental data. The idea behind this approach was that such near-impeller data are hardly affected by the rest of the vessel and therefore could be used throughout. Generally, this is not the case of course. Furthermore, this approach necessitates the availability of accurate experimental data, not only

with respect to the average velocity components, but also for k and ε. The latter variable in particular can hardly be measured directly. Nowadays, this approach is no longer used, also due to the steep increase in computer power which no longer urges for such drastic simplifications.

In those early days, when computer power was limited, often use was made of a symmetry assumption: each quarter of the vessel containing one of the four baffles at the vessel wall was supposed to behave identically; hence, a steady flow in the RANS approach was simulated in just a quarter vessel. Such strong simplifications are no longer in use. Precessing vortices moving around the vessel centerline contribute to flow unsteadiness and, therefore, exclude models that just assume flow steadiness or allow for domain reductions through geometrical symmetries. The most correct response to this flow unsteadiness is the concept of LES.

Later on, in 1994, novel options were introduced such as Sliding Mesh (SM) and Multiple Frames of Reference (MFR) in which the flow domain is divided into two parts, each with their own meshing; one mesh is connected to the stationary vessel wall and the other one to the revolving impeller. The interaction of the flow fields at either side of the interface between these two meshes requires delicate bookkeeping of fluxes and forces among cells moving with respect to one another at the interface. Of course, these methods are a drastic improvement over the black box description of the impeller swept area applied in the early days of stirred vessel CFD. The mesh associated with the impeller in SM is perfectly capable of simulating the unsteady flow around the impeller blades including the trailing vortices.

The MFR technique introduced by Luo *et al.* (1993, 1994) starts from a steady-state description of the flow field and therefore fits in RANS-based simulations only. The SM approach (e.g., Murthy *et al.*, 1994; Bakker *et al.*, 1997) is a fully transient method, also applicable in LES (see, e.g., Bakker *et al.*, 2000; Jahoda *et al.*, 2006; Gao and Min, 2006; Gao *et al.*, 2006). Yeoh *et al.* (2004a, b) adopted a Sliding and Deforming Mesh (SDM) technique in which the two grids do not only slide with respect to each other but also feel shear resulting in deforming interface cells. Keeping mass and momentum conserved in this technique requires bookkeeping somewhat different from that with the SM technique.

Generally, however, it is unclear what (with SM) the effect is of the position of the interface between stationary and moving meshes on the simulated unsteadiness of the overall flow in the vessel. In addition, simulations making use of SM and MFR may suffer from slower or poor convergence. Of course, the transient SM technique is more accurate, though at the cost of larger computer time consumption. Montante *et al.* (2006) even reported that MFR yielded unphysical findings, viz. a region of opposite swirl.

Harvey *et al.* (1995) and Harvey and Rogers (1996) proposed a multiblock impeller-fitted grid structure for dealing with the exact geometry of the impeller. The first of these two papers introduces an approximate steady-state method

that solves the viscous flow with the impeller at one position with respect to the baffles ignoring its relative motion, while the second paper is about an unsteady moving grid approach that now takes the relative motion of the impeller with respect to the baffles into account. This approach, however, never made it into to the turbulent-flow regime.

Ranade and Van den Akker (1994) and Ranade and Dommeti (1996) introduced a snapshot approach in which *the impeller was put in a standstill* and the revolving flow in the simulation was obtained by imposing velocity jets at one or more fixed positions of the impeller blades. At a first glance, realistic flow fields were obtained, energy dissipation levels and the total amount of energy dissipated being in the right order of magnitude. A more detailed assessment of this approach, however, reveals that the equations used are not invariant to the type coordinate transformation used. Furthermore, elementary turbulence theory (e.g., Tennekes and Lumley, 1972) indicates that, with a view to the flow field in the impeller swept volume, a jet issuing from the face of an impeller blade may not be equivalent to a wake behind an impeller blade, as jets and wakes obey different laws for their expansion in downstream direction. As a result, the shape of the impeller connected zones of high k and ε values may not be predicted confidently. Ranade's snapshot approach (still in use, see, e.g., Khopkar *et al*., 2006) discussed further on page 207 should therefore be abandoned, in spite of all explanations devoted to it (Ranade, 2002).

Applying Immersed or Embedded Boundary Methods (Mittal and Iaccarino, 2005) circumvents the whole issue of the friction between the more or less steady overall flow in the bulk of the vessel and the strongly transient character of the flow in the zone of the impeller. These methods are introduced below. In the context of a LES, Derksen and Van den Akker (1999) introduced a forcing technique for both the stationary vessel wall and the revolving impeller. They imposed no-slip boundary conditions at the revolving impeller and at the stationary tank wall (including baffles). To this purpose, they developed a specific control algorithm.

B. Curved Boundaries

In stirred vessels and static mixers the flow domain is bounded by complex boundaries due to the curvature of containing walls, the revolving impeller axis and/or static mixing elements.

While in the early days a staircase representation of a curved boundary in a cubic grid was quite common, commercial CFD software nowadays exploits boundary fitted meshing. The staircase representation usually was not a problem—in terms of mass conservation or of introducing artefacts such as additional small eddies—as long as the steps did not involve more than a single grid cell. The currently widely adopted boundary fitted meshing, i.e., generating body-conformal either structured or unstructured grids providing adequate

local resolution with a minimum but large number of grid cells, requires either commercial grid generating software or extensive coding (usually far beyond the reach of academic groups). The impact of a poor grid on accuracy and on convergence properties of the solver may not be underestimated.

Whenever a cubic grid is mandatory—either due to coding limitations from the part of academic groups or due to the inherent properties of, e.g., LB techniques—and a staircase approach is to be avoided (e.g., for a revolving impeller axis) one can take refuge to some immersed boundary method (see, e.g., Mittal and Iaccarino, 2005). One may distinguish between

- embedded boundary methods using cut cells: these methods adjust cell volume and face areas to the geometry of the body in the flow domain; while in a FV approach this method guarantees global and local conservation of mass and momentum, it creates problems in an explicit formulation of the FV scheme;
- immersed boundary methods exploiting boundary forcing methods: a boundary is simply treated as a force exerted or felt at the position of the boundary; this position may even be time dependent, e.g., in the case of a revolving impeller; and
- immersed boundary methods using ghost cells: ghost cells are boundary cells the centers of which are lying outside the flow domain; in this approach, values of variables in these ghost cells are required to satisfy, e.g., a Neumann boundary condition (velocity gradients normal to a wall zero, velocity component along a wall zero at the wall).

Which of the various immersed or embedded boundary methods is best—generally or for a particular case—is still an open question. Thornock and Smith (2005) introduced a Cell Adjusted Boundary Force Method for a stirred vessel. All methods proposed so far have their own pros and cons. Immersed boundary methods are also exploited in LB techniques (e.g., Derksen and Van den Akker, 1999). Rohde (2004) investigated the use of triangular facets for representing a spherical particle.

C. The Domain and the Grid

With a view to any simulation, a few important items have to be addressed. First of all, it has to be decided whether the flow to be simulated is 2-D, $2^{1/2}$-D, or 3-D. When the flow is, e.g., axis-symmetrical and steady, a 2-D simulation may suffice. For a flow field in which all variables, including the azimuthal velocity component, may not depend on the azimuthal coordinate, a $2^{1/2}$-D simulation may be most appropriate. Most other cases may require a full 3-D simulation. It is tempting to reduce the computational job by casting the 3-D flow field into a 2-D mode. The experience, however, is that in 2-D simulations the turbulent viscosity tends to be overestimated; in this way, the flow

may become more or less diffusion dominated and less capable of sustaining a transient behavior. Furthermore, between 2-D and 3-D, the wall to volume ratio is different, turbulence intensity may go down, and hydrodynamic stability may be affected. Of course, the above remarks apply to RANS-based simulations only, as LES are inherently transient and 3-D.

A second choice to be made relates to the size of the flow domain. It may be worthwhile to limit the calculational job by reducing the size of the flow domain, e.g., by identifying an axis or plane of symmetry, or, in a cylindrical vessel with baffles mounted on the wall, due to periodicity in the azimuthal direction. Commercial software accomplishes these choices by means of 'symmetry cells' and 'cyclic cells,' respectively; although such choices reduce the size of the simulation, they may eliminate the possibility of finding the real (asymmetric, unstable, or transient) 3-D flow field. The presence of feed pipes or drain or withdrawal pipes may also make the use of symmetry or cyclic cells impossible. Again, this issue only plays a role in RANS-type simulations.

A third issue is how many grid cells should be used for the domain size selected. In general, using more computational cells implies more detailed insight in the flow field as a result of the simulation, at the cost of longer CPU times (although sometimes convergence rate may increase as a result of increasing the number of grid cells.) This is a trade-off that is to be decided upon, each time a new flow field is to be simulated. In some cases, a stepwise approach may be pursued to zoom into a particular zone within a flow device (see, e.g., Stekelenburg *et al.*, 1994).

A fourth issue is the use of local grid refinement: many commercial codes offer this modality, often with unstructured grids. The rationale behind the idea of introducing local grid refinement techniques is that the grid is only refined in those parts of the calculation domain in which the flow exhibits strong spatial or temporal gradients. By doing so, one does not waste grid cells in parts of the domain where the flow does not vary significantly. Rohde *et al.* (2006) explored the use of a generic, mass-conservative local grid refinement technique within a LB technique. He successfully attempted this technique for various rather simple cases; so far, it has not been exploited in a cylindrical stirred vessel in which the flow would require a fine grid not only in the impeller swept region but also near to the baffles.

Anyhow, the result of any flow simulation should be grid independent, i.e., the flow field should not be different if a finer grid is used for the simulation. This test is to be carried out always and everywhere, and may really be described as a *conditio sine qua non*.

Finally, it is good to quote Shaw (1992, p. 227): 'the most important asset in a CFD analysis process is the analyst, who actually translates the engineering problem into a computational simulation, runs the CFD solver and analyzes the results. It is the skill of this person, or set of persons, that will determine whether all the hardware and software will be utilized in the best possible way and produce good quality results.' CFD is certainly not a panacea that may solve all

possible design and optimization problems. It rather is a tool that in the hands of a well-trained professional may provide valuable insights in the local phenomena and processes, which take place in (bio)reactors and all sorts of process equipment including mixing devices. CFD-simulations may provide a good starting point for a mechanistic description of operations such as blending, suspending solids, dispersing gas, and carrying out (bio)chemical reactions.

V. Simulations of Turbulent Flows in Stirred Vessels

When exploiting computational techniques for studying the mixing performance of stirred tanks and static mixers, the first question is how well the turbulent-flow field and the characteristic turbulence properties are predicted by the various forms of CFD discussed above. The different forms of CFD (RANS, LES, DNS) and the various strategies, turbulence models, and submodels used by them may suffer from a different degree of validity in the various mixing devices considered. The impact of a limited validity of the models used may vary from case to case. That is why validation of simulation results is still an urgent issue. Sometimes, the results of computational simulations just *look* qualitatively correct. It is important to check code performance by means of quantitative experimental data as to average quantities as well as local and transient fluctuations.

The next question then is whether the processes taking place inside this turbulent-flow field can be modeled with confidence. We will now first consider the first question.

A. Turbulence Properties

It is worthwhile to verify whether or not some basic assumptions of turbulence theory (local equilibrium between production and dissipation of turbulence, isotropy, homogeneous turbulence) which are used in modeling certain aspects of momentum transport via turbulent eddies are met with in stirred tanks. To be honest, at hardly any position in a stirred tank the production rate of turbulent kinetic energy balances the rate of its dissipation. Production of turbulence mainly takes place in the impeller swept volume, while a much larger part of the vessel takes part in dissipating the turbulence. In addition, the action of a revolving impeller and its interaction with nearby baffles turns the flow intrinsically unsteady. As a result, the turbulent flow in a stirred vessel is certainly not an equilibrium flow, as presumed in using, e.g., the Smagorinsky SGS model in LES.

Most RANS-based simulations make use of the k–ε model for taking into account the momentum transport due to the turbulent eddies. This model is an

eddy-viscosity model and as such it assumes isotropic turbulent transport. The question is whether *everywhere* in a stirred tank the turbulent flow is *locally* isotropic. This issue might have to be explained a bit further as 'local isotropy' should be distinguished from just 'isotropy.' Local isotropy means that the fluctuations can be modeled with an (isotropic) eddy viscosity, while isotropy has been defined as having the same fluctuation levels in the three coordinate directions. Local isotropy does not imply isotropy of the fluctuations: a k–ε model can predict nonisotropic fluctuations.

The question whether or not stirred tank flow is locally isotropic, may be investigated with the help of a LES which resolves a great deal of the Reynolds stresses. To this end, the Reynolds stress data are best presented in terms of the so-called anisotropy tensor a_{ij} and its invariants A_1, A_2, and A_3.

The anisotropy tensor is related to the turbulent stresses, of course, and is defined as

$$a_{ij} = \frac{\overline{u_i u_j}}{k} - \frac{2}{3}\delta_{ij} \tag{15}$$

Its first invariant A_1 is equal to zero by definition. The second and third invariants of this tensor are $A_2 = a_{ij}a_{ji}$ and $A_3 = a_{ij}a_{jk}a_{ki}$, respectively. The range of physically allowed values of A_2 and A_3 is bounded and represented by the so-called Lumley triangle in the (A_3, A_2) plane (Lumley, 1978). The distance $|A| = \sqrt{(A_2{}^2 + A_3{}^2)}$ from the isotropic state, i.e., from the origin ($A_2 = 0$, $A_3 = 0$), is a measure of the degree of anisotropy. See also Escudié and Liné (2006) for a more extensive discussion as to how to quantify and visualize how different from isotropic turbulence a stirred vessel is.

Phase-averaged values of $|A|$ in a plane midway between two baffles of a stirred tank have been plotted in Fig. 1 (from Hartmann *et al.*, 2004a) for two different SGS models (Smagorinsky and Voke, respectively) in LES carried out in a LB approach. The highest values, i.e., the strongest deviations from isotropy, occur in the impeller zone, in the boundary layers along wall and bottom of the tank, and at the separation points at the vessel wall from which the anisotropy is advected into the bulk flow. In the recirculation loops, the turbulent flow is more or less isotropic.

Fig. 2 (also from Hartmann *et al.*, 2004a) shows how the values of the invariants A_2 and A_3 found in a LES using a Smagorinsky SGS model are distributed within the Lumley triangle. Most but not all of the points are clustered in the lower part of this triangle. This implies that in a large part of a stirred tank the turbulent flow is more or less isotropic and the use of a turbulent viscosity and a k–ε model are permitted. On the whole, however, turbulent flow is not really isotropic. This may also explain why in RANS-based simulations turbulent kinetic energy levels generally are underestimated.

As far as ε is concerned: it is extremely difficult to measure its spatial distribution and its wide range of values experimentally. LES may provide an

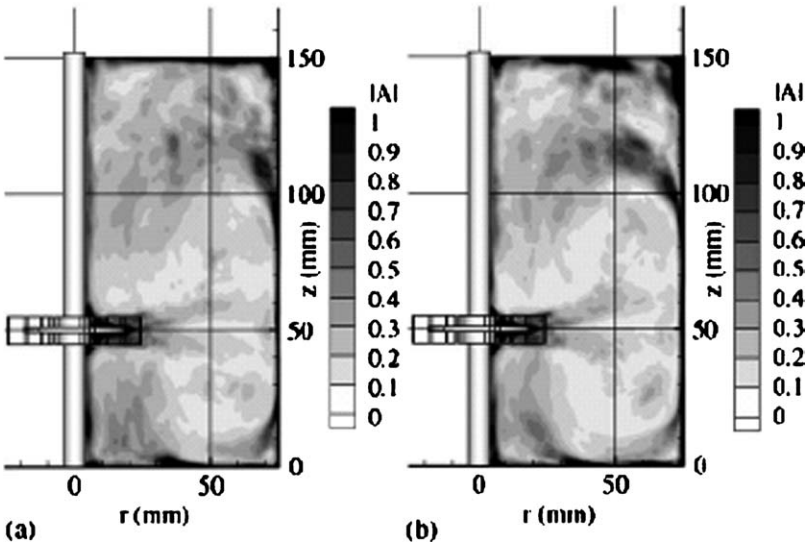

FIG. 1. Phase-averaged plots of the anisotropy distance $|A|$ in a plane midway between two baffles in a stirred vessel provided with a Rushton turbine, as obtained by means of LES, with two different SGS models: (a) the Smagorinsky model; (b) the Voke model. Reproduced with permission from Hartmann *et al.* (2004a).

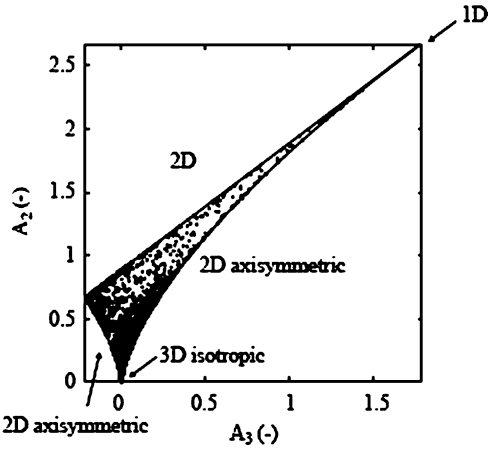

FIG. 2. This plot shows to which degree, according to a LES, the turbulence in a plane midway between two baffles in a stirred vessel provided with a Rushton turbine can be typified. For clarity, not all grid points in such a plane have been used for this plot. According to Lumley (1978), the borders represent different types of turbulent flows: 3-D isotropic turbulence, 2-d axis-symmetric turbulence, 2-D turbulence, and 1-D turbulence. Most but not all points are concentrated in the lower part of this Lumley triangle. Reproduced with permission from Hartmann *et al.* (2004a).

attractive alternative. Micheletti *et al.* (2004) present a valuable discussion on this issue.

B. Validation of Turbulent Flow Simulations

In view of the different requirements as to computer power, it is very worthwhile to compare the outcome of RANS and LES simulations mutually and/or with quantitative experimental data. Several authors have done this, e.g., Derksen and Van den Akker (1998, 1999), Derksen (2001), Lu *et al.* (2002), Ranade (2002), Derksen (2002b), and Yeoh *et al.* (2004a,b). In most cases, the experimental data have been obtained by means of Laser-Doppler Anemometry (LDA, or LDV): see, e.g., Yianneskis *et al.* (1987), Wu and Patterson (1989), Schäfer *et al.* (1997, 1998), and Derksen *et al.* (1999). In this review, we will mainly refer to the validation study due to Hartmann *et al.* (2004a).

In comparing RANS results and LES results with LDA data, the focus is first on the global, phase-averaged flow field: see Fig. 3 (from Hartmann *et al.*, 2004a) that relates to a plane midway between two baffles. The two types of simulations capture the dominant flow feature, viz. the two large circulation loops, more or less to the same extent. The RANS simulation better predicts the position of the point where the upper loop separates from the vessel wall. As far as turbulent kinetic energy (k) levels are concerned, k-values obtained in a LES relate to the resolved turbulent eddies. Hartmann *et al.* (2004a) argued that the SGS fluctuations hardly contribute to the k-levels. It is evident from Fig. 4 that the RANS simulation underestimates the kinetic energy levels created by the blades of the Rushton impeller. The same conclusion applies to phase-resolved kinetic energy data (see Fig. 5). The RANS simulation is hardly capable of catching the remainders of the trailing vortices created by the preceding impeller blade, while LES nicely reproduces this succession of vortices. Whenever one is interested in details of the turbulent-flow field because they may affect the performance of the mixing device, one should really consider carrying out a LES. The findings due to Yeoh *et al.* (2004a) are completely in line with this.

As long as the interest is in fields of averaged velocity components and in overall mixing patterns, RANS-based simulations may suffice. Examples of such satisfactory simulation results are plentiful, e.g., Marshall and Bakker (2004) and Montante *et al.* (2006). When, however, the interest is in the details of the turbulent-flow field and in processes affected by these details, LES is the option to be preferred. From the findings reproduced above and from the validation studies of Derksen and Van den Akker (1999) and Derksen (2001) the general conclusion is that, as long as the spatial resolution is sufficient, LB LES deliver results in excellent agreement with experimental turbulence data.

Large eddy simulations explicitly resolves the inherently unsteady character of the turbulent flow in a stirred tank into account, including the periodic phenomena associated with the motion of the impeller and their interaction with

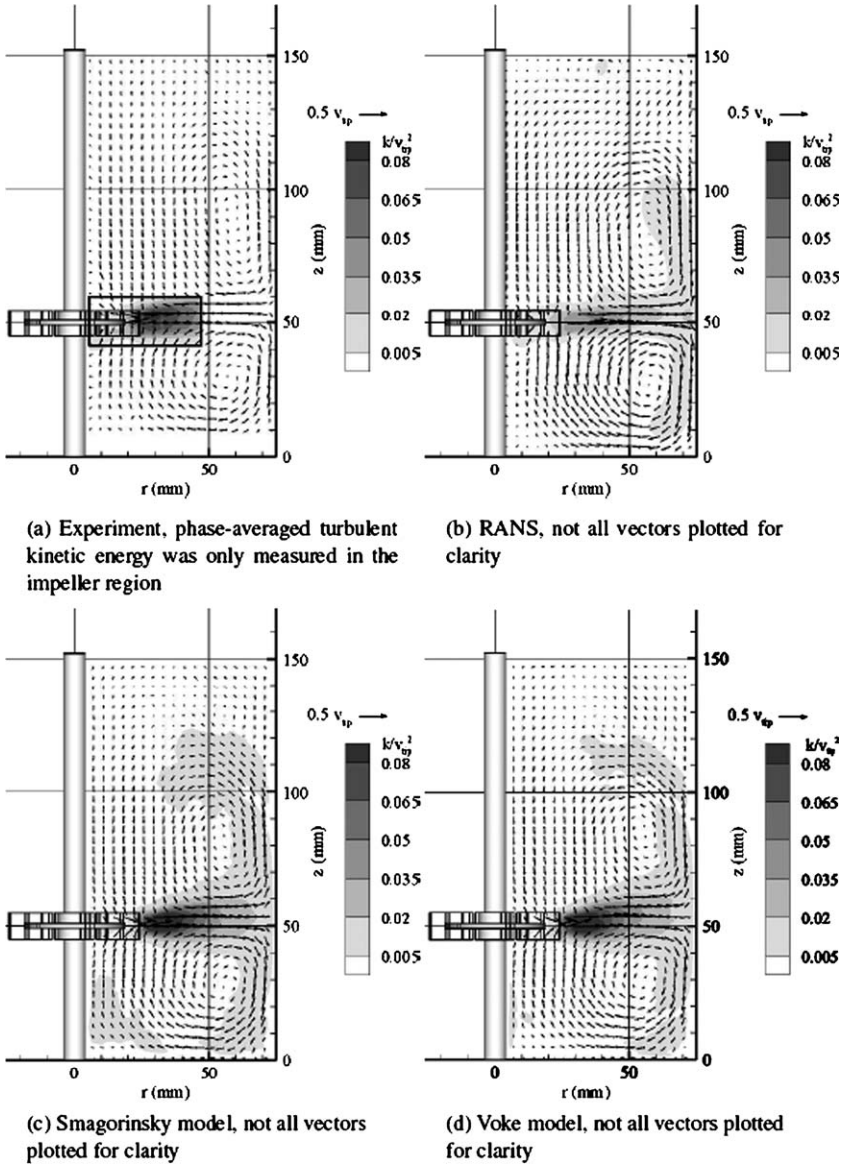

(a) Experiment, phase-averaged turbulent kinetic energy was only measured in the impeller region

(b) RANS, not all vectors plotted for clarity

(c) Smagorinsky model, not all vectors plotted for clarity

(d) Voke model, not all vectors plotted for clarity

FIG. 3. Velocity vector fields and levels of turbulent kinetic energy in a plane midway between two baffles in a stirred vessel, according to LDA data (a); a RANS-based simulation (b); and two LES (c) and (d). Reproduced with permission from Hartmann *et al.* (2004a).

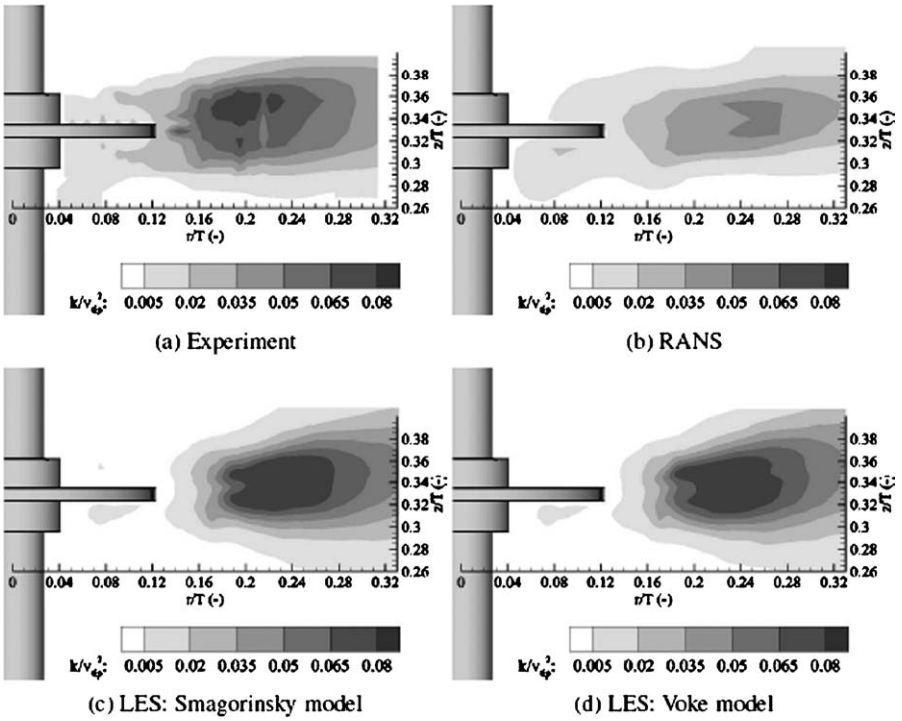

FIG. 4. Phase-averaged plots of turbulent kinetic energy in the vicinity of the Rushton impeller as found in different types of simulations as indicated. Reproduced with permission from Hartmann *et al.* (2004a).

the baffles. Global as well as subtle flow features are in *quantitative* agreement with experimental data. Typical examples of such a quantitative agreement are—for six-bladed Rushton turbines—the path along which the trailing vortices developing at the impeller blades are swept into the bulk of the tank as well as the turbulent kinetic energy levels in the wakes of the impeller blades; in a vessel equipped with a pitched-blade turbine, we could mention the primary and secondary recirculations in the phase-averaged flow field.

Derksen (2001) and Hartmann *et al.* (2004a) demonstrated that various choices in SGS modeling did not have a big impact on the quality of the flow field predictions. In addition, all these studies did not reveal a significant effect of the value of the Smagorinsky coefficient within the range 0.08–0.14.

One of the complications in stirred tank flows is the presence of macroinstabilities (i.e., low-frequency mean flow variations) that may affect the mixing performance. Various authors have distinguished between various types and investigated their occurrence and their frequencies under varying operating conditions and with several types of vessels and impellers (Yianneskis *et al.*, 1987; Haam *et al.*, 1992; Myers *et al.*, 1997; Hasal *et al.*, 2000; Nikiforaki *et al.*, 2002).

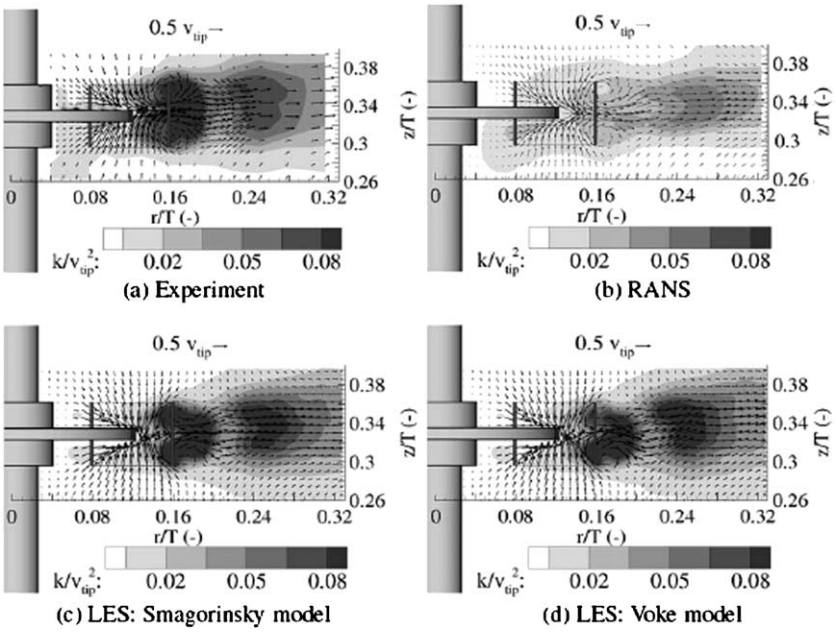

FIG. 5. Phase resolved plots of velocity vector field and turbulent kinetic energy in a plane 15° behind an impeller blade (obtained by sampling data only when the measuring point is at the specified position with respect to the impeller blades). Not all vectors have been plotted for clarity. Reproduced with permission from Hartmann *et al.* (2004a).

Roussinova *et al.* (2003) and Hartmann *et al.* (2004b) found that the LES methodology is excellently capable of reproducing various types of macroinstabilities. While Nikiforaki *et al.* (2002) experimentally found precessing frequencies in the range 0.013–0.018 N, the LES of Hartmann *et al.* (2004b) arrived at 0.0228 and 0.0255 N as the dominant frequencies, where N stands for the impeller speed (in number of revolutions/s). The discrepancy between experimental and numerical frequencies is a challenge for further improving particularly the SGS-model and some numerical settings.

VI. Operations and Processes in Stirred Vessels

In simulating physical operations carried out in stirred vessels, generally one has the choice between a Lagrangian approach and a Eulerian description. While the former approach is based on tracking the paths of many individual fluid elements or dispersed-phase particles, the latter exploits the continuum concept. The two approaches offer different vistas on the operations and require different computational capabilities. Which of the two approaches is most

suited is hard to say: it depends on the details of the issue of interest and on the computational power available.

In whichever approach, the common denominator of most operations in stirred vessels is the common notion that the rate ε of dissipation of turbulent kinetic energy is a reliable measure for the effect of the turbulent-flow characteristics on the operations of interest such as carrying out chemical reactions, suspending solids, or dispersing bubbles. As this ε may be conceived as a concentration of a passive tracer, i.e., in terms of W/kg rather than of m^2/s^3, the spatial variations in ε may be calculated by means of a usual transport equation.

In the context of the RANS-methodology, this ε is also required for solving the spatial distributions of the velocity components, while in LES ε just serves the purpose of providing a basis for modeling the operation(s) of interest.

Even when the number of grid cells in a LB LES simulation of a stirred vessel 1.1 m^3 in size amounts to some 36×10^6 grid cells, this implies a cell size, or grid spacing, of 5 mm only. Even a cell size of just a few millimeters makes clear that substantial parts of the transport of heat and species as well as all chemical reactions take place at scales smaller than those resolved by the flow simulation. In other words: concentrations of species and temperature still vary and fluctuate within a cell size. The description of chemical reactions and the transport of heat and species therefore ask for subtle approaches to these SGS fluctuations.

A. Mixing and Blending

One of the most crucial (design) parameters in blending two miscible liquids or distributing a particular miscible addition over a heel of liquid is the so-called mixing time, i.e., the time needed to achieve complete homogenization or a predetermined degree of homogeneity (see, e.g., Grenville and Nienow, 2004). In this review, the focus is on blending operations carried out with low viscosity fluids in the turbulent regime.

Kramers *et al.* (1953) were among the first to study mixing times as a function of baffle position and impeller rotational speed. Results of several experimental studies have been combined into empirical correlations relevant to industrial applications (Procházka and Landau, 1961; Hoogendoorn and Den Hartog, 1967; Sano and Usui, 1985; Grenville, 1992; Ruszkowski, 1994; Nienow, 1997). Grenville and Nienow (2004) present a concise review as to such correlations.

Bouwmans (1992; see also Bouwmans *et al.*, 1997) used a particle tracking technique in a RANS flow field to estimate trajectories of neutral and buoyant additions, to construct *Poincaré* sections of additions crossing specific horizontal cross-sectional planes, to predict probabilities of surfacing for buoyant additions, and to mimic the temporal response of conductivity probes.

Exploiting the Eulerian point of view, Ranade *et al.* (1991) was one of the first to simulate mixing times for a vessel provided with a pitched blade turbine; in

this early work, the impeller swept area was still modeled as a black box just delivering inlet conditions for the turbulent flow in the remainder of the vessel. Various authors (Osman and Varley, 1999; Jaworski *et al*., 2000; Bujalski *et al*., 2002) used SM or MFR techniques in RANS-based simulations for Rushton turbines driven flow combined with species transport equations to predict mixing times, but arrived at values 2–3 times higher than the experimental values. This is in line with the findings for Rushton turbines that in such RANS-based simulations turbulence levels are underpredicted and that mixing across the central plane of the discharge plane is poorly reproduced. Montante and Magelli (2004) studied a homogenization process in a baffled vessel stirred with various sets of Rushton turbines; while effects of varying impeller number and spacing were correctly forecasted, a very low turbulent Schmidt number had to be adopted for obtaining good quantitative agreement in terms of tracer response curves. RANS-based simulations of mixing in tanks provided with pitched blade turbines prove to underpredict mixing times, probably owing to mesoscale concentration fluctuations not really reproduced by the simulation.

All these findings of disappointing quantitative agreement with experimental data stem from the inherent drawback of the RANS-approach that there is no clear distinction between the turbulent fluctuations modeled by the Reynolds stresses and (mesoscale) fluctuations. In LES, however, the distinction between resolved and unresolved turbulence is clear and relates to the cell size of the computational grid chosen.

The LES methodology has recently been applied in a number of studies simulating in a stirred tank the mixing in response to the addition of a tracer. Yeoh *et al*. (2004a) carried out an FV-simulation that matched the experimental set-up of Lee (1995); the focus of their study is on mixing patterns, on traces of concentrations at certain monitoring points, and on a comparison of predicted mixing time with correlations from literature. Hartmann (2005) and Hartmann *et al*. (2006) coupled an FV solver for the species transport to an LB flow solver. In his study, different from Yeoh *et al*. (2005), the passive scalar is injected at zero speed to avoid an effect of jet mixing on mixing times. Hartmann aimed at reproducing the experiments of Distelhoff *et al*. (1997) and focused on the effect of impeller size and 'injection' position on mixing time. A sample of his results is presented in Fig. 6. For the time being, the results due to Hartmann still suffer from an unphysical mass increase caused by the current implementation of his novel immersed boundary method using ghost cells.

Comparative studies on simulating mixing times by means of the traditional RANS approach and the more sophisticated LES are due to Gao and Min (2006), Gao *et al*. (2006), and Jahoda *et al*. (2006). They all show that RANS-based simulations fail in reproducing the transient responses of probes monitoring the local tracer concentrations, while LES is able to mimic the experimental traces quite accurately (see Fig. 7, from Jahoda *et al*., 2006). The latter traces strongly resemble those presented by Hartmann (2005) and Hartmann *et al*. (2006).

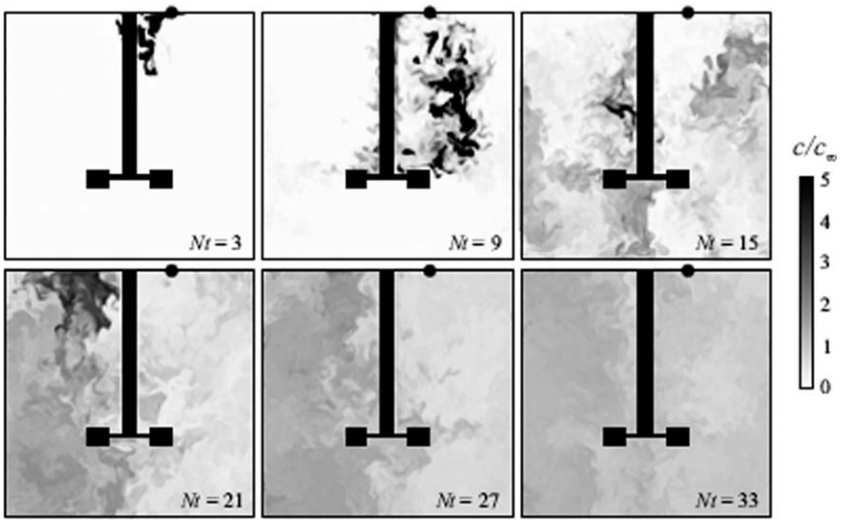

FIG. 6. A sample of Hartmann's results (2005). The tracer is injected (with zero speed) at the top of the tank in a plane midway between two baffles (black dot in the plots). The concentration fields shown are also in the midway baffle plane. T/D = 3, c_∞ denotes the final uniform concentration.

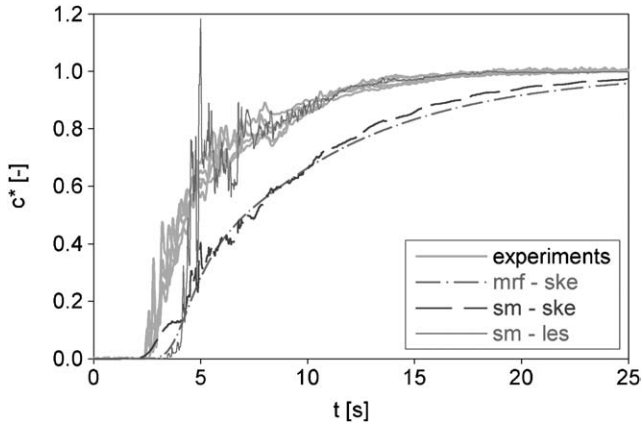

FIG. 7. Time traces of normalized concentration as 'seen' by a probe in the lower part of a vessel in simulations of a mixing time experiment. The vessel is provided with two Pitched Blade Turbines. Three different types of simulations are shown, where 'ske' stands for a standard k–ε simulation and 'sm', 'mrf,' and 'les' have the usual meaning. Reproduced with permission from Jahoda *et al.* (2006).

B. SUSPENDING SOLIDS

An important class of stirred tank applications involves suspending discrete solid particles in a continuous liquid phase where the turbulent-liquid-flow

generated by the impeller induces particle motion and should prevent sedimentation. Such suspensions are for instance encountered in industrial crystallization and in catalytic slurry reactors. The usual procedure in designing such processes is making use of the Zwietering correlation (1956). Note that in the NAMF Handbook of Mixing, Chapter 10 on Solid-Liquid Mixing does not refer to any CFD results.

Although the Zwietering correlation provides valuable guidance to chemical engineers in, e.g., solving practical engineering problems and dealing with scaling-up issues, at a more fundamental level there are many unresolved issues such as:

- What is actually going on at the particle scale (in terms of, e.g., heat and mass transfer, or mechanical load on particles as a result of particle–particle and particle–impeller collisions) and how are these microscale events affected by the larger-scale phenomena?
- On the reverse, how does the presence of particles affect local and global flow features in the vessel such as the vortex structure in the vicinity of the impeller, power consumption, circulation and mixing times, and the spatial distribution of turbulence quantities; more specifically: colliding particles have an impact on the liquid's turbulence (Ten Cate *et al.*, 2004) while local particle concentrations affect the effective (slurry) viscosity which may be useful in the macroflow simulations?

Most of these issues may best be studied by DNS, while other can better be tackled by LES. Anyhow, RANS-based simulations are not very suited to this purpose as the turbulence in the RANS-approach is not resolved at all but just modeled. Below, typical DNS-, LES-, and RANS-based simulations of solids suspensions will be reviewed in succession.

1. A Direct Numerical Simulations Approach

In view of secondary nucleation in crystallizers, Ten Cate *et al.* (2004) were interested in finding out locally about the frequencies of particle collisions in a suspension under the action of the turbulence of the liquid. To this end, they performed a DNS of a particle suspension in a periodic box subject to forced turbulent-flow conditions. In their DNS, the flow field around and between the interacting and colliding particles is fully resolved, while the particles are allowed to rotate in response to the surrounding turbulent-flow field.

Ten Cate *et al.* (2004) were able to learn from their DNS about the mutual effect of microscale (particle scale) events and phenomena at the macroscale: the particle collisions are brought about by the turbulence, and the particles affect the turbulence. Energy spectra confirmed that the particles generate fluid motion at length scales of the order of the particle size. This results in a strong increase in the rate of energy dissipation at these length scales and in a decrease

of the turbulence at larger length scales. All these details were obtained just by restricting the DNS to a small periodic box. Details of their approach will be dealt with further on; a typical result is Fig. 12.

2. *Results of Large Eddy Simulations*

Derksen (2003), on the contrary, was interested in simulating the process of solids suspension in a stirred tank; to this end, he tracked particles in the whole tank in a Lagrangian sense, considering the particles as point particles and not resolving the detailed flow field between the particles. In other words, Derksen applied a more superficial view on the particle suspension by dropping details, and was rewarded with a picture of the full tank: see Fig. 8. Yet, Derksen was able to track just over 6.7 million particles, to include effects such as particle rotation, particle–particle collisions, particle–impeller collisions and even two-way coupling, and to include fluid–particle interaction forces such as the *Saffman* force, the *Magnus* force, and forces due to stress gradients. Tracking all these particles was done in a turbulent-flow field obtained via an LB LES.

Derksen (2006a) continued along this line of approach and—by means of a clever strategy—mimicked the long-time behavior of solids suspension in an unbaffled tall stirred tank equipped with four hydrofoil impellers (Lightnin® A310). The time span covered by his LES amounted to some 20,000 impeller revolutions (some 20 min). Running a LES for a Reynolds number of 1.6×10^5 over the entire time span is not an option, and for that reason a particular flow

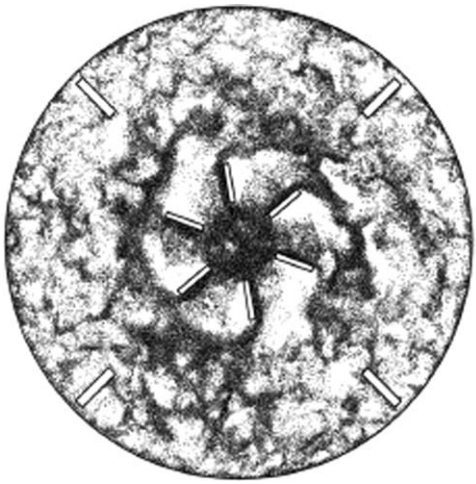

FIG. 8. This is a snapshot of a spatial particle distribution. The plane shown is the horizontal cross-section just below the disc of a Rushton turbine in a flat-bottomed stirred tank. The impeller revolves in the counter clockwise direction. Particle size is some 0.468 mm; $\mathrm{Re} = 1.5\cdots \times 10^5$; volume fraction amounts to 3.6%; number of particles tracked in the simulation just over 6.7 million. Reproduced with permission from Derksen (2003).

time series of sufficient length is stored and repeatedly played for tracking the paths of 20,000 particles 0.33 mm in diameter and with a density of 2,450 kg/m^3. The advantage of this approach is that use is made of the highly resolved flow information of the LES. The simulations of the particle response to the typical flow field created by the four impellers showed the counterintuitive behavior observed by Pinelli *et al.* (2001): almost all solid particles rise to the top of the tank.

3. *Results of Reynolds Averaged Navier–Stokes Simulations*

A very different type of CFD-simulation results are those due to, e.g., Montante and Magelli (2005) who studied solids suspension in stirred tanks by means of two-fluid CFD simulations, i.e., a RANS-type of Euler–Euler simulations. These authors tested two commercial CFD codes, viz. *FLUENT* 6.0 and *CFX*4, for various formulations of the two-fluid model, of the fluid–particle interaction force, and of the k–ε turbulence model for multiphase flow. Montante and Magelli just focused on predicting axial profiles of the solids concentration for three baffled stirred tanks agitated with single and multiple impellers; they evaluated the effect of the various model formulations on these profiles and compared their various predicted curves with experimental data. This type of simulation delivers data relevant for engineering purposes of limited scope and depth only.

In this context, one component of the phase interaction force may need separate discussion: the drag force. While most authors use the Schiller–Nauman equation

$$C_D = \frac{24}{\mathrm{Re}_p}\left(1.0 + 0.15\mathrm{Re}_p^{0.687}\right) \tag{16}$$

for the relation between particle drag coefficient and the particle Reynolds number (see, e.g., Ranade, 2002, or Derksen, 2003). Brucato *et al.* (1998), however, reported experimental data showing that free stream turbulence may significantly increase particle drag coefficients. They proposed a novel correlation for predicting the effect of free stream turbulence on the particle drag coefficient:

$$\frac{C_{Dt} - C_D}{C_D} = 8.76 \cdot 10^{-4}\left(\frac{d_p}{\eta_K}\right)^3 \tag{17}$$

in which $C_{D\,t}$ denotes the particle drag coefficient in a turbulent flow and C_D stands for the usual particle drag coefficient as given by Eq. (16). Equation (17) implies that the drag coefficient for particles the size of which is smaller than or comparable with that of the smallest turbulent eddies (represented by the local *Kolmogorov* length scale η_K) is hardly affected by free-stream turbulence, while the fluid-mechanical interaction of larger particles with turbulent eddies becomes significant and leads to an increase of particle drag.

Montante *et al.* (2000), Micale *et al.* (2000), and Montante and Magelli (2005) incorporated this novel correlation into their two-fluid simulations of solids suspension in stirred vessels and arrived at pretty good agreement with experimental data. These authors claim that this correlation due to Brucato *et al.* (1998) plays an essential role in arriving at this good agreement: introducing the turbulence effect reduces the tendency of the larger particles to collect in the bottom part of the vessel. One may argue, however, that the introduction of a higher particle drag coefficient is rather artificial and just compensates for shortcomings in the two-fluid formulation used, such as ignoring all other components of the phase interaction force. By the way, Micale *et al.* (2004) in simulating particle suspension height ignored this effect of free stream turbulence and identified it as a second-order effect only.

In some way, introducing an increased particle drag by means of Eq. (17) resembles the earlier proposal raised by Bakker and Van den Akker (1994b) to increase viscosity in the particle Reynolds number due to turbulence (in agreement with the very old conclusion due to Boussinesq, see Frisch, 1995) with the view of increasing the particle drag coefficient and eventually the bubble hold-up in the vessel. Lane *et al.* (2000) compared the two approaches for an aerated stirred vessel and found neither proposal to yield a correct spatial gas distribution.

In addition, it is dubious whether this new correlation due to Brucato *et al.* (1998) should be used in any Euler–Lagrangian approach and in LES which take at least part of the effect of the turbulence on the particle motion into account in a different way. So far, the LES due to Derksen (2003, 2006a) did not need a modified particle drag coefficient to attain agreement with experimental data. Anyhow, the need of modifying particle drag coefficient in some way illustrates the shortcomings of the current RANS-based two-fluid approach of two-phase flow in stirred vessels.

The present author wonders whether, due to its very nature (particularly, the various assumptions as to averaging and the various modeling uncertainties), a RANS-based two-fluid approach is suited for reproducing the details of solids suspension in a stirred vessel. May be we should be satisfied with the gross predictions of the current RANS methods and turn to LES for the details of those processes which are dominated by the spatially distributed turbulence. It is really a valid question how long we should keep trying and improving the RANS two-fluid approach as now the increased computer power brings the much more sophisticated LES within reach.

C. Dissolving Solids

Properly simulating a dissolution process of solid particles in a stirred vessel operated in the turbulent-flow regime urges for a very detailed simulation of the turbulent-flow field itself. Just reproducing the overall flow pattern by means of

a RANS-type of simulation is not sufficient! Our estimate is that a two-fluid simulation (on the basis of RANS) yields too rough an approximation of the process. The dissolution process may too strongly depend on the heavily fluctuating flow and concentration fields around particles which—as the result of the presence and action of eddies of various scales—may move chaotically with respect to one another while being advected through the vessel.

One really may need an inherently transient LES to capture all these details. The finer the grid for such a LES, the more reliably the local transient conditions may be taken into account in reproducing this turbulent mass transfer process (while ignoring the issue of supplying the heat for the dissolution which may also depend on a proper representation of the turbulent-flow field). An additional important issue is how many particles have to be tracked for a proper representation of the transient spatial distribution of the particles over the vessel.

Hartmann *et al.* (2006) reported very detailed simulation results (see also Hartmann, 2005) (Fig. 9). Their LB simulation was restricted to a lab-scale vessel 10 L in size only for which 240^3 lattice cells a bit smaller than 1 mm^2 were used; the temporal resolution was 25 μs only. A set of 7 million mono-disperse spherical particles 0.3 mm in size was released in the upper 10% part of the vessel. At the moment of release, the local volume fraction amounted to 10%. The particle properties were those of calcium chloride. The simulation was carried out on 30 parallel processors of an SGI Altrix 3700 system and required for 6 weeks for 100 impeller revolutions.

Figure 9 presents some typical results for the spatial distribution of the dissolving particles, their sizes, and their size distribution. Initially, the particles respond to the centrifugal forces in the vortices and collect at the outer regions of the vortices, giving rise to streaky patterns. The dissolution process results in decreasing particle sizes and, hence, in decreasing inertia to the effect that gradually they start behaving like fluid tracers. Overall, the solids and scalar concentrations become more homogeneous in the course of the dissolution process. The simulation even predicts that a plot of the *Sauter* mean diameter d_{32} vs. time may exhibit a minimum (not shown here).

D. Precipitation and Crystallization

The counterparts of dissolving particles are the processes of precipitation and crystallization the description and simulation of which involve several additional aspects however. First of all, the interest in commercial operations often relates to the average particle size and the particle size distribution at the completion of the (batch) operation. In precipitation reactors, particle sizes strongly depend on the (variations in the) local concentrations of the reactants, this dependence being quite complicated because of the nonlinear interactions of fluctuations in velocities, reactant concentrations, and temperature.

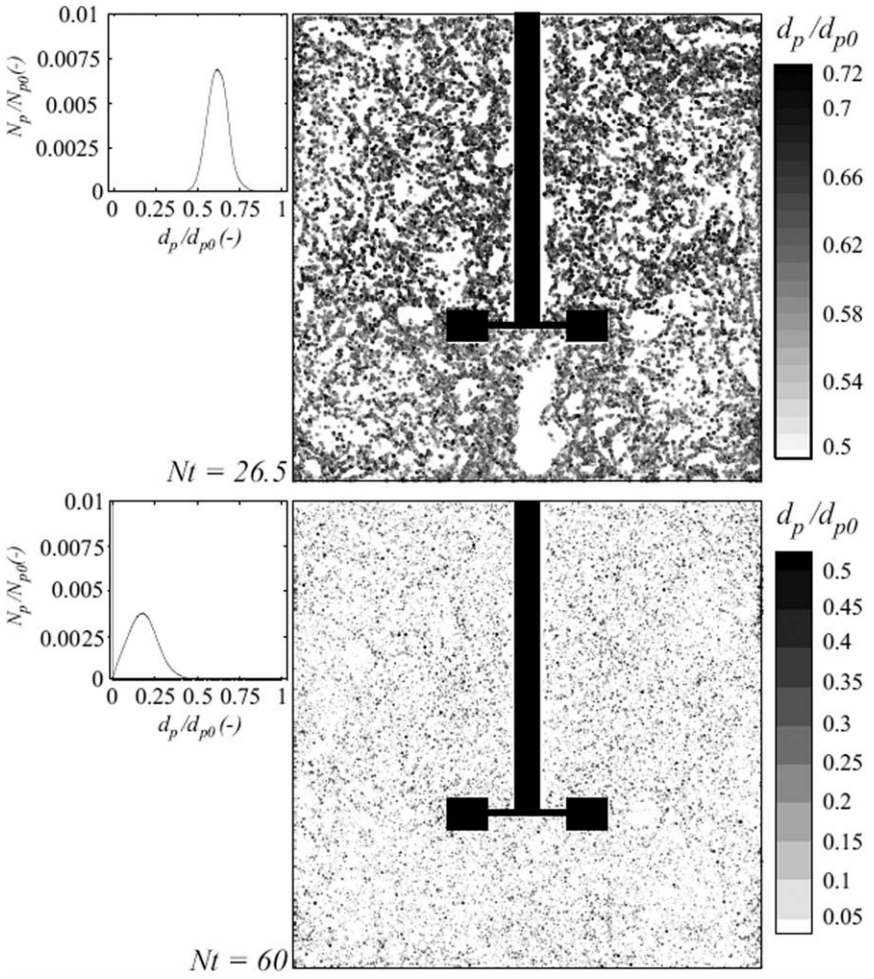

FIG. 9. Snapshots of particle sizes and their spatial distribution in a vertical midway baffle plane at two moments in time, along with the pertinent respective overall particle size distributions. The diameter of the particles is enlarged by a factor of 10 for reasons of clarity. Grey colors represent particle size with respect to the original particle size. Reproduced with permission from Hartmann (2005).

The same applies to crystallizers, in which particle sizes and particle number concentrations not only depend on nucleation and growth from supersaturated mother liquid, but are also affected by shear-dominated agglomeration and by secondary nucleation as a result of particle–particle and particle–impeller collisions. Some of the subprocesses involved may be limited to specific and different parts of the vessel: e.g., nucleation may be restricted to a flame-like region around the outlet of a feed pipe (Van Leeuwen, 1998). In addition, in

many cases, many more product properties are relevant, such as color, texture, and particle morphology.

Gradually, the insight is growing that all these properties are not only affected by the averaged process conditions in reactor or crystallizer, but also by their spatial and temporal variations felt by the particles during their stay in and on their pathways through the vessel (see, e.g., Rielly and Marquis, 2001). The first response of modelers was to introduce compartmental modeling (Van Leeuwen, 1998; Bermingham *et al.*, 1998; Ten Cate *et al.*, 2000): the vessel is divided into several compartments, each compartment being considered as (more or less) ideally mixed and described in terms of averaged values of the process parameters such as temperature, concentrations, and rate of turbulent kinetic energy dissipation; these averaged values may vary strongly from compartment to compartment. Although this approach is an improvement over the traditional method of lumping all variations into a single average value, an important problem still is how to decide on the number and size of the compartments. Carrying out RANS-type simulations would be an option for selecting proper compartmentalization on a case-to-case basis.

Seckler *et al.* (1995), Van Leeuwen *et al.* (1996), and Wei and Garside (1997) were among the first to exploit commercial CFD codes (*FLUENT* and *PHOENICS*) for simulating precipitation reactors (of a particular simplified design) by adding to their codes some simple precipitation kinetics, i.e., relations for nucleation and particle growth. Van Leeuwen *et al.* (1996) included the first four moments of the crystal size distribution in their simulations. Van Leeuwen (1998) was the first to study precipitation in a stirred vessel; among other things, he explored the option for extending his RANS-type simulations with a routine involving the use of PDFs to account for variations in the species concentrations (see one of the next sections on chemical reactors). He did not arrive at a satisfactory agreement with experimental data.

As discussed in several of the above sections, LES is much better suited to represent the spatial and temporal variations in a turbulent-flow field. Of course, this is very relevant in precipitation reactors and crystallizers where the particle formation is a highly nonlinear process. Progress is being made in developing LES including detailed models (e.g., PDFs, or methods of moments) for specific reactive systems (e.g., combustion, polymerization) under specific conditions in simple geometries (e.g., tubular reactors): see also one of the next sections on chemical reactors. In turbulent agitated precipitation reactors and crystallizers, however, mixing is so intense and complex and so heavily dominated by the revolving impeller that so far no one has succeeded in simulating the full process of nucleation, particle growth, agglomeration, and particle break-up and in arriving at a reasonable prediction of the eventual particle size distribution.

Certain isolated aspects of precipitation and crystallization which have successfully been studied by means of LES, are discussed below to illustrate the progress being made in the field of precipitation and crystallization. The LB

technique exploited in these studies is very helpful, since LB easily allows parallel computing and the related computational acceleration. These detailed studies may make a similar simulation possible as presented above for a dissolution process.

1. *Agglomeration*

Hollander (2002) and Hollander *et al.* (2001a,b, 2003) studied agglomeration in a stirred vessel by adding a single transport equation for the particle number concentration m_0 (actually, the first moment of the particle size distribution)

$$\frac{\partial m_0}{\partial t} + \nabla \cdot (\tilde{\mathbf{v}} m_0) = -\frac{1}{2}\beta_0 m_0^2 \tag{18}$$

Note that the particle diffusion term is ignored, just like particle dispersion due to SGS motions (this was found justified in a separate simulation). The shape of the sink term in the right-hand term of this equation is due to Von Smoluchowski (1917) while the local value of the agglomeration kernel β_0 is assumed to depend on the local 3-D shear rate according to a proposition due to Mumtaz *et al.* (1997).

This additional Eq. (18) was discretized at the same resolution as the flow equations, typical grids comprising 120^3 and 180^3 nodes. At every time step, the local particle concentration is transported within the resolved flow field. Furthermore, the local flow conditions yield an effective 3-D shear rate that can be used for estimating the local agglomeration rate constant β_0. Fig. 10 (from Hollander *et al.*, 2003) presents both instantaneous and time-averaged spatial distributions of β_0 in vessels agitated by two different impellers; color versions of these plots can be found in Hollander (2002) and in Hollander *et al.* (2003).

The results of these simulations confirm the suspicion of a large spread in β_0-values across the vessel. Furthermore, the simulations show that agglomeration does not occur in the impeller region, as the hydrodynamic conditions (shear!) are too severe for agglomerates to survive. A bulk region can be defined in which agglomeration conditions are beneficial. Due to the typical structure of the flow (i.e., trailing vortices, large-scale turbulent motion), the vessel contains large gradients in agglomeration rates. It is this effect that causes large differences in the local particle consumption rate and leaves the vessel with a very uneven distribution in particle concentration.

Fig. 11 presents the results of some 30 simulations for various conditions and two impeller types in terms of the mean agglomeration rate constant observed in the various simulations vs. the vessel-averaged shear rate found in the simulations. The simulations all started from the dotted curve for relating local agglomeration rate constant to local shear rate. A clear decrease in the maximum of β_0 as well as a shift toward higher average shear rates was found which are caused by the local nature of the nonlinear flow interactions only. These

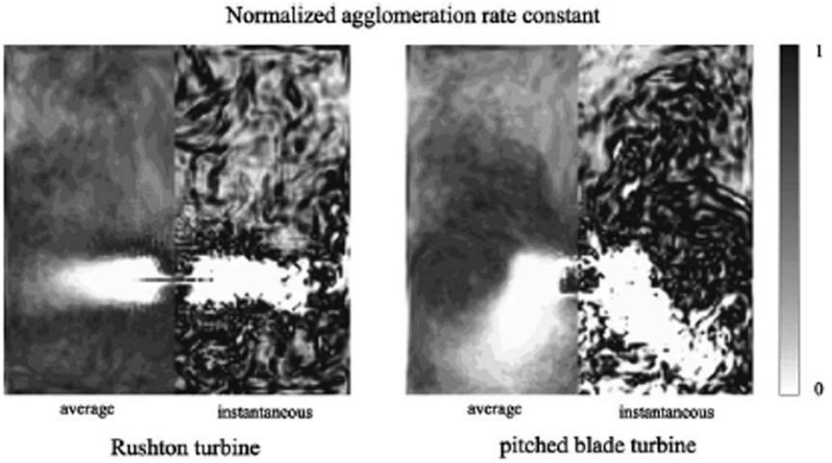

FIG. 10. Results of LES-based simulations of an agglomeration process in two vessels: one agitated by a Rushton turbine (left) and one agitated by a Pitched Blade Turbine (right). The two plots show the agglomeration rate constant β_0 normalized by the maximum value, in a vertical cross-sectional plane midway between two baffles and through the center of the vessel. Each of the two plots consists of two parts: the right-hand parts present instantaneous snapshots; the left-hand parts present spatial distributions of time-averaged values after 50 impeller revolutions. Reproduced with permission from Hollander *et al*. (2003).

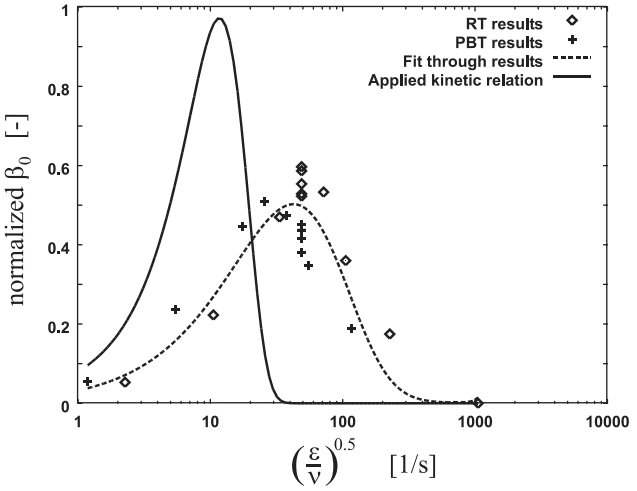

FIG. 11. The discrepancy between the original kinetic relation due to Mumtaz *et al*. (1997) and the observed relation between mean agglomeration rate constant β_0 and volume-averaged shear rate. Symbols refer to individual numerical simulations (LES). RT stands for Rushton Turbine, PBT for Pitched Blade Turbine. Reproduced with permission from Hollander *et al*. (2001b).

nonlinear effects may play an important role in our mediocre understanding of the scale-up behavior of agglomeration processes in stirred vessels.

The computational demands for Hollander's simulations (in 2000) were typically of the order of 1 CPU week on a PentiumIII/500 MHz at 400 MB of memory per run. The computer code was fully parallelized and was run on a 12 CPU Beowulf cluster.

2. *Colliding Particles*

Finally, Ten Cate *et al.* (2001) studied secondary nucleation as a result of crystal–crystal collisions by means of a two-step approach. The first step involved a LES of the complete crystallizer in which the liquid phase (typically containing 10–20%v of solids) is treated as a single phase with a homogeneous density and viscosity. (In principle, density and viscosity may be allowed to vary locally in the simulation, by invoking the help of a particle dispersion routine (e.g., Liu, 1999) and coupling the resulting particle concentrations back to a SGS model to modify the local values of density and viscosity.) The spatial grid resolution (some 5.0 mm) used by Ten Cate typically was at least 10 times the crystal size; the grid comprised some 36 million cells.

The second step in Ten Cate's two-step approach was to focus on crystal–crystal interaction by means of an explicit two-phase DNS of the turbulent suspension that completely resolves the translational and rotational motions and collisions of the spherical particles plus the turbulence of the liquid between the particles. The particle motions are driven by the turbulent flow and the particles affect the turbulent flow of the liquid in between. When particles approach one another down to a distance smaller than the grid spacing, lubrication theory is exploited to bridge the gap between them.

At the start of a simulation, the particles (up to 3,900) are placed randomly, without mutual contact and with zero velocity, into a fully developed turbulent single-phase flow field in a periodic box. This starting situation is subjected to a precalculated force field; this forcing involves a divergence-free white-noise signal, distributed over the wave number domain as a Gaussian distribution about a desired wave number, with a characteristic root mean square velocity and a characteristic length scale. In this way, turbulent conditions are generated which accurately recover a priori set values such as the *Kolmogorov* length scale, the integral length scale, and the integral time scale, derived from the LES at some position somewhere in the crystallizer. For details, the reader is referred to Ten Cate (2002) and Ten Cate *et al.* (2004).

The evolution of the two-phase turbulence depends on the initial random position of the particles, the motion of which modifies the turbulent-flow field directly. These DNS are therefore a nice example of two-way coupling between the two phases: see Fig. 12. From these DNS, detailed knowledge can be derived as to the frequency of the particle–particle collisions and the forces involved

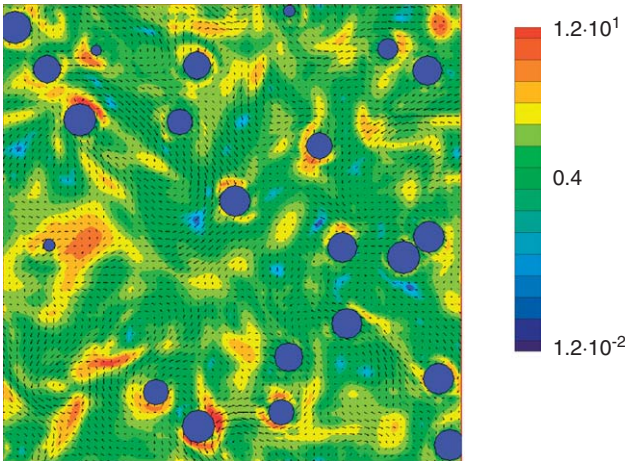

FIG. 12. Snapshot from a two-phase DNS of colliding particles in an originally fully developed turbulent flow of liquid in a periodic 3-D box with spectral forcing of the turbulence. The particles (in blue) have been plotted at their position and are intersected by the plane of view. The arrows denote the instantaneous flow field, the colors relate to the logarithmic value of the nondimensional rate of energy dissipation.

(as a function of local conditions in a crystallizer) which may yield quantitative data on secondary nucleation (fragmentation of crystals due to collisions).

VII. Stirred Gas–Liquid and Liquid–Liquid Dispersions

Similar problems as encountered in simulating agitated suspensions also play a role in agitated gas–liquid and liquid–liquid systems. Again, there is the dilemma whether to use a Lagrangian approach or to apply a two-fluid, Euler–Euler, model. Then, there is again the question of one-way coupling vs. two-way coupling. Thirdly, the issue of taking the particle size distribution into account (yes or no) should be addressed. Further, particle–particle interaction may not be ignored in many cases, and then the additional problem is coalescence of bubbles or droplets, and their break-up. All these issues have not been tackled simultaneously in the past, not in the least because of computational limitations.

Furthermore, the physics of the interaction between turbulence and bubbles in the complex flow of a stirred vessel, with its implications for coalescence and break-up of bubbles and drops, is still far from being understood. Up to now, simple correlations are available for scale-up of industrial processes; generally, these correlations have been derived in experimental investigations focusing on the eventual mean drop diameter and the drop size distributions as brought

about by the power input (mainly) via the impeller given the fluid properties (e.g., Colenbrander, 2000).

In the 1980s, Issa and Gosman (1981), Pericleous and Patel (1987), and Trägårdh (1988) made the first attempts to simulate aerated stirred vessels computationally. Their results were rather approximate indeed, and were not validated by means of experimental data.

A. Bakker's GHOST! Code

In the early 1990s, Bakker and Van den Akker (1991, 1994) introduced an approximate but effective Euler–Euler approach (see also A. Bakker's PhD Thesis, 1992): on the basis of a single-phase RANS flow field calculated by *FLUENT*, a code named *GHOST!* calculated local and averaged values of bubble size d_b, gas hold-up α, and specific mass transfer rate $k_l a$.

Their *GHOST!*-code essentially consisted of a mass balance for the gas, a transport equation for the bubble number density n_b, and a force balance for a single bubble, respectively, which run as

$$\nabla \cdot (\bar{\alpha}\bar{\mathbf{u}}) - \nabla \cdot (\nabla(D\bar{\alpha})) = \bar{S}_g \tag{19}$$

$$\frac{\partial n_b}{\partial t} + \nabla \cdot (n_b \mathbf{u}) = \omega(n_{b\infty} - n_b) + \frac{\bar{S}_g}{V_{b,in}} \tag{20}$$

$$-\rho_l V_b \frac{w^2}{r}\hat{r} - \rho_l g V_b \hat{z} = C_D \frac{1}{2}\rho_l |\mathbf{u_s}|\mathbf{u_s}\frac{\pi}{4}d_b^2 \tag{21}$$

respectively. Of course, the variables n_b, d_b, and α are interrelated. The second term in the mass balance, Eq. (19) stands for the extra transport of the bubbles due to the larger turbulent eddies; usually, this turbulent transport is taken into account by a separate term in the momentum balance for the dispersed phase which, however, in Bakker's approach is replaced by the simple force balance, Eq. (21), for a single bubble. The coefficient ω in the transport equation for n_b is just a relaxation parameter that stands for the rate at which n_b responds to the local turbulence, i.e., adapts—either by coalescence (in the bulk of the stirred vessel) or by bubble break-up (in the impeller swept domain of the vessel)—to the local equilibrium number density $n_{b\infty}$ The latter variable corresponds to the local maximum stable bubble size $d_{b\infty}$ which—according to Hinze (1955)—depends on the local value of the specific rate of energy dissipation ε:

$$d_{b\infty} = C_{b\infty}\left(12\frac{\sigma}{\rho_l}\right)^{3/5}\varepsilon^{-2/5} \tag{22}$$

Bakker increased the local values of ε as obtained with *FLUENT* by a contribution related to the slip velocity of the bubbles. Working with a single

relaxation parameter ω is a phenomenological description avoiding detailed relations for coalescence and bubble break-up.

The Eulerian gas velocity field required in both the mass balance and the above transport equation for n_b is found by an approximate method: first, the complete field of liquid velocities obtained with *FLUENT* is adapted downward because the power draw is smaller under gassed conditions; next, in a very simple way of one-way coupling, the bubble velocity calculated from the above force balance is just added to this adapted liquid velocity field. This procedure makes a momentum balance for the bubble phase redundant; this saves a lot of computational effort.

Finally, Bakker and Van den Akker calculated local values for the specific mass transfer rate $k_l a$, by estimating local k_l-values from local values of the *Kolmogorov* time scale $\sqrt{(\nu/\varepsilon)}$ and by deriving local values of the specific interfacial area a from local values for bubble size and bubble hold-up.

In spite of all the simplifications Bakker and Van den Akker applied and given the black box approach for the impeller swept domain, their simulations resulted in values for the bubble size just below the liquid surface, overall hold-up, and average $k_l a$ values which are in good agreement with their experimental data (see Table II). The major step forward they made was the acquisition of the different spatial distributions of average bubble size (see Fig. 13), bubble hold-up and $k_l a$ as effected by three common impeller types. As a matter of fact, their approach may be restricted to low values of the gas hold-up.

B. Venneker's DAWN Code

Venneker *et al.* (2002) extended the *GHOST!* approach due to Bakker and Van den Akker (1994b) by replacing the single transport equation for the

TABLE II

Computational and Experimental Results for Overall Hold-up ∃, Size $\langle d_{B,OUT} \rangle$ of the Bubbles Leaving the Liquid Heel, and Overall Specific Mass Transfer Rate $k_L A$ (from: Bakker, 1992)

S. no.		∝ (%)		$\langle d_{b,out} \rangle$ (mm)		$k_l a$ (l/s)	
		Exp.	Sim	Exp	Sim	Exp	Sim
1	DT	4.7±0.2	4.9	3.25	2.91	0.038	0.038
2	A315	4.6±0.2	4.2	3.76	3.59	0.035	0.036
3	A315	4.8±0.2	4.3		3.82	0.038	0.036
4	PBT	4.1±0.3	4.1	3.44	3.39	0.036	0.037
5	PBT	1.1±0.3	1.0		2.00	0.011	0.013

Note: The respective impellers used are a classical Rushton turbine (DT), a hydrofoil impeller (A315) manufactured by Lightnin, and a Pitched Blade impeller (PBT). The cases 1 through 4 all relate to a superficial gas rate of 3.6 mm/s only, with impeller speeds varying between 5 and 10/s (gas flow numbers between 0.01 and 0.02); cases 2 and 3 differ in sparger size and position.

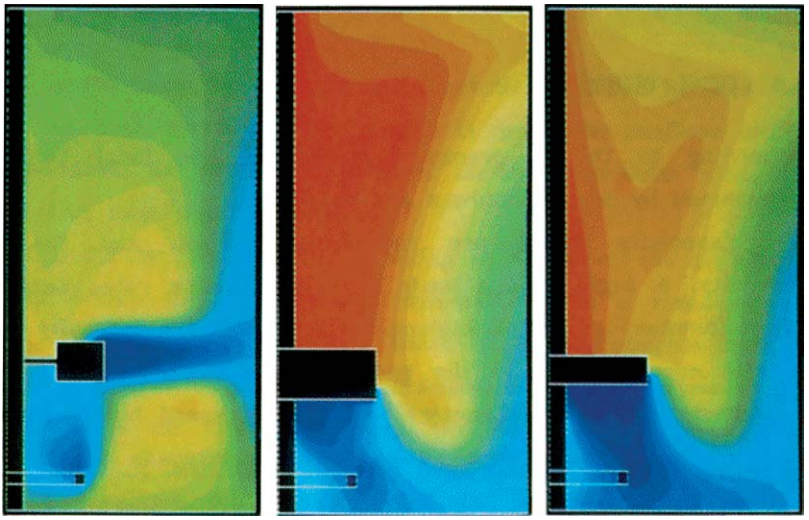

FIG. 13. Spatial distributions of bubble size in three vessels agitated by different impellers: a classical Rushton turbine (DT), a hydrofoil impeller (A315) manufactured by Lightnin, and a Pitched Blade Impeller (PBT). The gas flow numbers in these simulations are in the range 0.01–0.02. These simulation results have been obtained by using GHOST! Reproduced with permission from Bakker (1992).

bubble number density including the effective relaxation parameter ω by a number of population balance equations. Actually, these population balance equations are convective-diffusive transport equations for the bubble number density in a specific bubble size class and include separate birth and death terms which take coalescence and break-up into account. In addition, the procedure for adapting the liquid flow field to the lower power draw under gassed conditions has been improved on the basis of experimental findings due to Roušar and Van den Akker (1994). For the rest, the same approximations are made as in *GHOST!* with respect to gas velocities, rate of energy dissipation, and specific mass transfer rate.

Venneker *et al.* (2002) used as many as 20 bubble size classes in the bubble size range from 0.25 to some 20 mm. Just like *GHOST!*, their in-house code named *DAWN* builds upon a liquid-only velocity field obtained with *FLUENT*, now with an anisotropic Reynolds Stress Model (RSM) for the turbulent momentum transport. To allow for the drastic increase in computational burden associated with using 20 population balance equations, the 3-D *FLUENT* flow field is averaged azimuthally into a 2-D flow field (Venneker, 1999, used a less elegant simplification!)

The agreement between simulation results and experimental data is encouraging (see Fig. 14), although the simulation gives higher hold-up values in the upper part of the vessel while the overall hold-up is lower in the simulation than

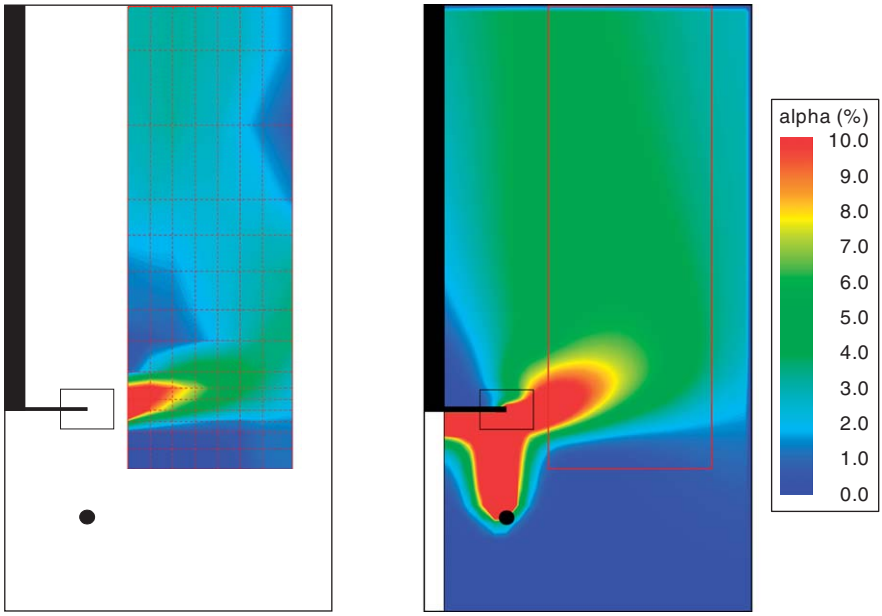

FIG. 14. Spatial distribution of the gas hold-up in a turbulent stirred vessel filled with a 0.075% Keltrol solution in water and agitated by a Rushton turbine: (a) experimental data obtained by means of an optical probe; (b) computational result from DAWN. Overall hold-up amounts to some 3.1% in the simulation and 3.7% in the experiment. Reproduced with permission from Venneker (1999), improved.

in the experiment. The latter discrepancy may be due to the use of optical probes overlooking bubbles smaller than, say, 1 mm.Venneker *et al.* (2002) present some more comparisons between computational and experimental results. One should realize, however, that for validation purposes hardly any detailed experimental data as to bubble size distributions in stirred vessels are available. This same shortage of experimental data hampers the assessment of the so-called MUltiple-SIze Group approach *MUSIG* due to Lo (2000) as incorporated in the commercial CFD code *CFX*.

C. Further Simulations

In comparison with Bakker and Van den Akker (1994b) and Venneker *et al.* (2002), Khopkar *et al.* (2005) applied a more sophisticated two-fluid approach including a standard k–ε turbulence model. Using the incorrect snapshot approach due to Ranade (2002), their simulation results (for gas flow numbers being 4 times higher than those of Bakker and Van den Akker, 1994b) still exhibit major discrepancies with respect to experimental data. One of the

striking features is that their liquid velocities even in the outflow of the Rushton impeller are pretty much overestimated in the simulation, may be due to the use of the snapshot approach (*cf.* the dicussion on page 180). The spatial distributions of gas hold-up found in the simulations are compared with experimental data obtained by means of computed tomography (CT); there is substantial room for improvement (see Fig. 15) in spite of the much more sophisticated type of simulation. The paper due to Gentric *et al.* (2005) exploits several features and options of the two-fluid mode of the commercial code *STAR-CD* and illustrates its capabilities in comparing the mixing performance of two industrial mixing vessels, but does not present validation by means of experimental data.

The combination of two-phase flow, turbulence, and a revolving impeller poses tremendous simulation problems and still requires excessive computer time or power. While in bubble columns and gas lift loops population balances are used with some success (see, e.g., Wang *et al.*, 2006), the flow field in a stirred tank is so much more complicated and turbulent and dominated by the revolving impeller that implementing them in stirred vessel simulations still causes serious convergence problems. Laakkonen *et al.* (2006) reduced such problems by restricting his simulation to a multiblock approach subdividing the stirred vessel into just 23 ideally mixed subregions: this approach actually is a kind of network of zone approach (see also, e.g., Hristov *et al.*, 2004, who even used 36,000 zones) extended with population balances and may not be named CFD indeed. The use of the so-called Quadrature Method of Moments (QMOM) has been suggested as a proper tool for combining population balances with CFD (Marchisio *et al.*, 2003), but so far has not been used for simulating gassed stirred tanks.

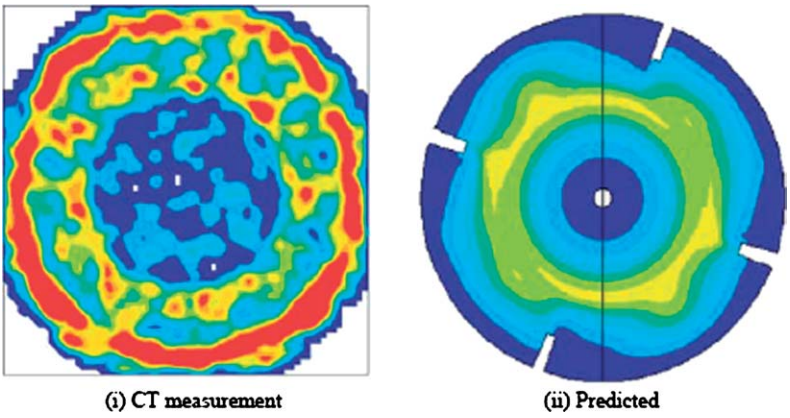

FIG. 15. Comparison of simulated and experimental gas hold-up distribution in a horizontal plane 10 cm above the bottom of the vessel. The gas flow number amounts to 0.084. Reproduced with permission from Khopkar *et al.* (2005).

D. A Promising Prospect

Just like in the context of simulating solids suspension, one may wonder whether much may be expected from just sticking to the two-fluid approach combined with population balances. A better way ahead might rather be to combine population balances with LES, while proper relations for the various kernels used for describing coalescence and break-up processes could be determined from DNS of periodic boxes comprising a certain number of bubbles (or drops). The latter simulations would serve to study the detailed response of bubbles or drops to the ambient turbulent flow.

An attractive framework for investigating these phenomena is provided by Derksen (2006b) who carried out DNS of liquid–liquid dispersions in a 3-D periodic box. Derksen investigated the response of a turbulent dispersion of droplets to a history comprising first a rapidly increasing turbulent activity, then a quasi-steady situation of high turbulence intensity and finally a rapid decay in turbulence intensity; this history may be equivalent to what a fluid package experiences during its passage through the impeller stream. Again, Derksen applied a particular LB method for mimicking the two phases. The drop size distribution and the *Sauter* mean diameter were tracked in time. Furthermore, the presence of the droplets affected the turbulence spectrum because of the small-scale fluid motions induced by the droplets, on the analogy of the interaction between solid particles and turbulence in the work of Portela and Oliemans (2003) and Ten Cate *et al*. (2004).

VIII. Chemical Reactors

So far, most (stirred) chemical reactors have been designed and scaled up by traditional methods exploiting simple concepts—such as 'continuous stirred tank reactor' and residence time distribution—and scale-up rules involving usually a single dimensionless number such as the (mixing) Damköhler number being the ratio of the turbulent macrotime scale to the characteristic reaction time scale. In addition, various types of local mixing times and their ratios are used to characterize or categorize the interaction of mixing and chemical reactions at scale-up (Patterson *et al*., 2004).

These methods hardly take spatial distributions of velocity field and chemical species or transient phenomena into account, although most chemical reactors are operated in the turbulent regime and/or a multiphase flow mode. As a result, yield and selectivity of commercial chemical reactors often deviate from the values at their laboratory or pilot-scale prototypes. Scale-up of many chemical reactors, in particular the multiphase types, is still surrounded by a fame of mystery indeed. Another problem relates to the occurrence of thermal runaways due to hot spots as a result of poor local mixing effects.

Patterson (1985) presented a concise review of the early developments in computational modeling of second-order chemical reactions and of more complicated and multiple reaction sets which are affected by an intermediate rate of local turbulent mixing. At that moment in time, closing the cross-correlation terms stemming from the turbulent fluctuations by means of micromixing models was still in its infancy. He also just hinted on the use of PDFs. Furthermore, the limited computer power of those days kept detailed simulations and their assessment impossible. Stirred vessels in particular were too difficult a type of flow devices to allow for application of rigorous CFD techniques, although some attempts were made with a very small number of zones or mixing segments only.

A. Mechanistic Micromixing Models

In the 1980s, Bourne along with a long series of co-workers at ETH Zurich developed a mechanistic micromixing approach in which lamellar structures were central. His lamellar structures represent the small flow structures of the size of the *Kolmogorov* length scale within which molecular diffusion is the mechanism bringing the chemical species into the intimate contact required for a chemical reaction. The best reference might be two papers due to Baldyga and Bourne (1984a, b).

Such lamellar structures have also been described and modeled by Ranz (1979) and Ottino (1980) in the context of chemical reactions in *laminar* flows. In Bourne's micromixing models for chemical reactors operated in the *turbulent*-flow regime, various assumptions are raised as to the engulfment, the deformation, and the lifetime of these lamellar structures which, along with the diffusion of the reacting species, all affect the yield of the chemical reactions taking place within these structures. Actually, a CDR equation—see Eq. (13)—is solved explicitly for a chemical species within a single Kolmogorov eddy. The most appealing models Baldyga and Bourne proposed for the evolution of such eddies are the Strain (*St*) Model, the Shear (*Sh*) Model, the Engulfment-Deformation-Diffusion (*EDD*) model, and then the simpler Engulfment (*E*) model. Bourne applied his technique to various sets of competing parallel or consecutive model reactions each carried out in a fed batch reactor.

In the 1990s, Bakker and Van den Akker (1994, 1996)—see also R.A. Bakker's PhD thesis (1996)—continued this mechanistic modeling approach by attempting a completely deterministic description of the 3-D small-scale flow field in which the chemical reactions take place at the pace the various species meet. Starting point is a lamellar structure of layers intermittently containing the species involved in the reaction. These authors conceived such small-scale structures as *Cylindrical Stretched Vortex* (*CSV*) tubes being strained in the direction of their axis and—as a result—shrinking in size in a plane normal to

their axis. Such *CSV* tubes showed up around 1990 in several studies exploiting DNS of turbulent flows in a periodic box. The evolution of a *CSV* tube during its lifetime can be found by means of an analytical solution of the vorticity equation. For the parameters typical of the turbulent-flow field in a stirred reactor, however, the vorticity distribution does not result in substantial winding of material lines during the pertinent short time scales. As a result, the main effect of the stretching of the *CSV* is just the exponential shrinking rate of more or less flat, only slightly curling material layers.

Consequently, Bakker (1996) described the concentration evolution of a *single* layer subjected to the vorticity field of a single *CSV* by means of a one-dimensional differential equation where both the nondimensional time and the nondimensional spatial coordinate contain the exponential shrinking rate. In this respect, the *CSV* approach differs from the various Bourne models in which the successive generation of several *multiple*-layer stacks is required and vortex age is a crucial element.

B. A Lagrangian Approach

In addition, Bakker and Van den Akker (1994, 1996) were the first to track the path such structures follow in the turbulent-flow field of a fed batch reactor computationally. This is extremely relevant as both vortex age (in Bourne's multiple-layer models) and *Kolmogorov* length scale strongly depend on the spatially strongly varying ε. Precisely this latter variable exhibits a very inhomogeneous spatial distribution that only can be estimated by means of CFD. The idea is that during the microscale process of mixing and reaction the macroflow field advects the reaction zone throughout the reactor, thereby exposing the zone to regions of varying ε. The flow field and the spatial ε-distribution were obtained via a RANS-type of simulation (*FLUENT*), while the tracking was done by means of a Discrete Random Walk approach. (It should be kept in mind that at the time of their simulations LES was not really an option yet!) In addition to their own *CSV* model, Bakker and Van den Akker also validated some of Bourne's micromixing models.

Some typical results from their simulations are presented in Fig. 16 in which the yield X_Q of the product Q from the slow reaction of a set of two competitive reactions in a fed batch reactor has been plotted vs. impeller speed for two micromixing models, viz. their own *CSV* model and Bourne's *EDD* model; their simulation results are compared with experimental data from Bourne and Yu (1991). For the cases shown, the *CSV* model may perform better than Bourne's *EDD* model, in particular when A is fed near to the impeller where mixing is most intense.

An alternative but similar approach (Akiti and Armenante, 2004) is to define the reaction zones (or blobs) as a separate phase distinct for the ambient fluid

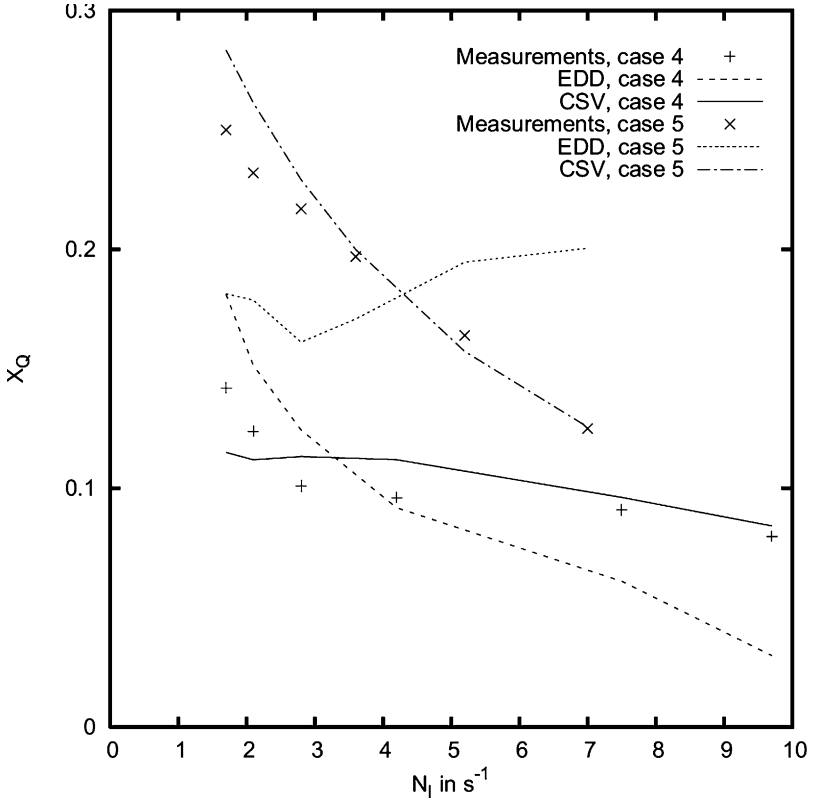

FIG. 16. The yield X_Q of the product Q of the slower reaction of a set of two competitive parallel reactions in a fed batch reactor plotted vs. impeller speed (in /s). The experimental data are due to Bourne and Yu (1991); the crosses refer to feeding reactant A at the top of the vessel, while the diamonds refer to feeding more closely to the impeller. The various types of lines refer to simulations as specified in the legend. Reproduced with permission from R. A. Bakker (1996).

and to track these reaction zones by means of a *Volume-of-Fluid* (VOF) technique, which may be conceived being a pseudo-multiphase model, originally designed by Hirt and Nichols (1981). Rather than a k–ε model, Akiti and Armenante used a RSM model to reproduce the turbulence characteristics of the flow field needed for the tracking procedure.

The most important drawback of using a Lagrangian approach for simulating (micro) mixing in chemical reactors is that some model is required for describing the formation of the *Kolmogorov*-scale flow structures at some (which?) distance from the mouth of the feed tube. This so-called feed discretization, aimed at defining the starting conditions (size, number, concentrations) for the lamellar structures, may have an unknown impact on the eventual yield.

C. A Eulerian Probabilistic Approach

An alternative approach (e.g., Patterson, 1985; Ranade, 2002) is the Eulerian type of simulation that makes use of a CDR equation—see Eq. (13)—for each of the chemical species involved. While resolution of the turbulent flow down to the *Kolmogorov* length scale already is far beyond computational capabilities, one certainly has to revert to modeling the species transport in liquid systems in which the *Batchelor* length scale is smaller than the *Kolmogorov* length scale by at least one order of magnitude: see Eq. (14). Hence, both in RANS simulations and in LES, species concentrations and temperature still fluctuate within a computational cell. Consequently, the description of chemical reactions and the transport of heat and species in a chemical reactor ask for subtle approaches as to the SGS fluctuations.

In order to obtain a realistic estimate for the reaction rate, the joint distribution of the reactants at the smallest turbulent scales is required. Any model disregarding this joint distribution may lead to an erroneous estimate of the reaction rate. For instance, filtering the reaction term, on the analogy of the LES filter for the fluid flow, would result in an over-prediction of the reaction rate due to the segregation at the subgrid scales. It may be just due to peculiar operating or mixing conditions when, such as in the *FLUENT* simulations reported on page 845 of Patterson *et al.* (2004), CFD simulations ignoring SGS fluctuations result in yield predictions close to experimental data. The value of the *Damköhler* number, denoting the ratio of the turbulent macrotime scale to the characteristic reaction time scale, plays an important role as well.

During the years, quite some proposals have been raised as to closure equations in the CDR equations for the spatial species distributions. These closure equations relate to the correlation terms in general and to the SGS fluctuations in species concentrations in particular. These proposals substantially differ in degree of sophistication. Patterson *et al.* (2004) present several examples of closure models which were reasonably successful in reproducing a particular set of experimental data. This, however, does not necessarily say something about their universal applicability. Bakker and Fasano (1993) applied the so-called *Magnussen* model and arrived at reasonable yield predictions for a competitive-consecutive reaction system in a stirred reactor (see also Marshall and Bakker, 2004). This *Magnussen* model, originally derived for combustion, locally calculates several reaction rates as a function of both mean concentrations and turbulence levels and then selects the lower rate for the source term in the CDR equation.

Particular attention is to be paid to closure models exploiting various types of PDFs such as beta, presumed, or full PDFs (e.g., Baldyga, 1994; Fox, 1996, 2003; Ranade, 2002). While PDFs have successfully been exploited for describing chemical reactions in turbulent flames, tubular reactors (Baldyga and Henczka, 1997), and a Taylor-Couette reactor (Marchisio and Barresi, 2003), they have never been used successfully in stirred reactors so far.

D. A Promising Prospect

At the end of this review on chemical reactors, special room is reserved for a very promising approach, although this approach, too, has not yet been applied for simulating a stirred chemical reactor. Van Vliet *et al.* (2001, 2005) exploited an elegant probabilistic approach (see also Van Vliet, 2003), where the PDF methodology incorporates the joint scalar information by solving the transport equation for the full joint scalar PDF (Pope, 1985). In this way, the second-order and thus nonlinear reaction terms in the CDR equation are kept in closed form, making further modeling of the chemical reaction term redundant.

In order to implement the PDF equations into a LES context, a filtered version of the PDF equation is required, usually denoted as 'filtered density function' (FDF). Although the LES filtering operation implies that SGS modeling has to be taken into account in order to capture micromixing effects, the reaction term remains closed in the FDF formulation. Van Vliet *et al.* (2001) showed that the sensitivity to the *Damköhler* number of the yield of competitive parallel reactions in isotropic homogeneous turbulence is qualitatively well predicted by FDF/LES. They applied the method for calculating the selectivity for a set of competing reactions in a tubular reactor at $\mathrm{Re} = 4{,}000$.

Although this LES/FDF methodology is a promising technique, the (current) drawback is the high computational costs involved to obtain a numerical solution of the FDF transport equation. In the above study due to Van Vliet (2003), the LES fluid transport was computed with the help of an LB solver on a 5×10^6 computational grid. Solving a transport equation for the joint PDF of the chemical species is most effectively done in a Lagrangian Monte-Carlo (MC) manner: the chemical composition of the flow as a function of time and space is represented by a collection of fictitious particles that are randomly released in the flow domain and that carry with them the full chemical composition. The assembly of MC particles is tracked through physical and chemical space by a set of stochastic ordinary differential equations, where the random term represents diffusion. These equations need closure as to the way the particles interact with their direct chemical environment, more specifically for the scalar energy dissipation rate. The model used is the rather common Interaction by Exchange with the Mean (IEM) model in which a mixing frequency describes the mixing at SGS.

Van Vliet *et al.* (2005) tracked 1×10^8 computational nodes to obtain a stochastic solution of their FDF equations. In order to deal with the high computational costs, the code was run in parallel on a Linux cluster of 11 dual AMD Athlon (TM) MP 1800+processors. In this way, about one 'turbulent macro time scale' (or 8,000 computational steps) per 2 days was computed.

Van Vliet *et al.* (2004, 2006) investigated the formation of hot spots and reactor efficiency in various geometrical configurations of a tubular reactor for manufacturing Low-Density Polyethylene (LDPE) by means of the above

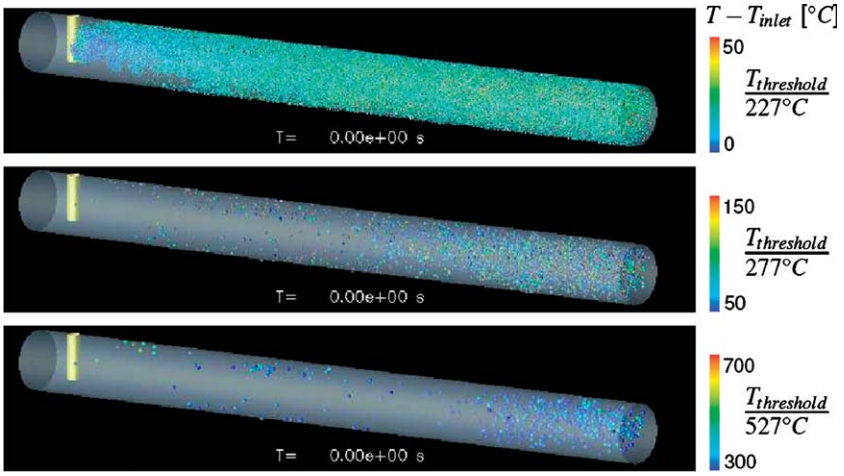

FIG. 17. Three different representations (using increasing temperature thresholds) of hot spots in a tubular LDPE reactor as found by the LES/FDF-methodology due to Van Vliet *et al.* (2004).

LES/FDF-approach. An 'In situ Adaptive Tabulation' (ISAT) technique (due to Pope) was used to greatly reduce (by a factor of 5) the CPU time needed to solve the set of stiff differential equations describing the fast LDPE kinetics. Fig. 17 shows some of the results of interest: the occurrence of hot spots in the tubular LDPE reactor provided with some feed pipe through which the initiator (peroxide) is supplied. The 2004-simulations were carried out on 34 CPU's (3 GHz) with 34 GB shared memory, but still required 34 h per macroflow time scale; they served as a demo of the method. The 2006-simulations then demonstrated the impact of installing mixing promoters and of varying the inlet temperature of the initiator added.

The above simulations as to the occurrence of hot spots once more illustrate the power and promises of LES over RANS-type simulations. The hot spots can never be found by means of a RANS-type of simulation. The same technique was used by Van Vliet *et al.* (2006) to study the influence of the injector geometry and inlet temperature on product quality and process efficiency in the LDPE reactor. On the contrary, the RANS-based simulations due to R. A. Bakker and Van den Akker (1994, 1996) were pretty much suited to arrive at yield predictions for a fed batch reactor as a whole.

So far, to the best of our knowledge, the above LES/FDF-approach has not been applied to stirred chemical reactors in which the turbulent-flow field is far more complex than in a tubular reactor. This LES/FDF-approach, however, may be the way to go, as it provides highly detailed information on turbulent reactive flows with the usage of a minimum of modeling assumptions. Although the high computational demands make LES/FDF simulations currently accessible to academic research groups only, the continued exponential growth of

computer resources will make them a versatile tool for process and geometry optimization of turbulent reactive flows in the process industries.

IX. Summary and Outlook

The above review has shown that 20 years of developing CFD-techniques has yielded us substantial simulation capabilities for studying and predicting mixing under turbulent conditions.

The start in the 1980s was slow and with much trial and error. In the early 1990s, we had to be content with RANS-based simulations on—speaking afterwards—coarse grids of limited size only. With increasing computer power and memory becoming available at lower cost, finer and larger grids offered the potential of getting more detailed pictures, among other things via DNS. LES entered the mixing scene, although their proliferation suffered from slow convergence of the FV solvers. In the late 1990s, however, LB solvers entered the mixing field and, owing to being faster and better geared to parallellization, made LES much more attractive and viable.

A. The Various Computational Fluid Dynamics Options

Nowadays, it is therefore essential to distinguish between the various main CFD options for dealing with turbulent mixing issues, viz.

- RANS simulations: usually exploiting some k–ε turbulence model, intended for global information on the average flow field and the global transport phenomena in full-scale process equipment, with additional output (of limited confidence level) on spatial distributions of k and ε;
- DNS simulations: delivering fully resolved transient fields of velocities and other variables in either a flow domain of limited size under laminar or very moderately turbulent flow conditions or in a periodic box with some prescribed turbulence level;
- LES: with some model of the SGS flow and transport phenomena, suited for reproducing—at the level of the grid cell size—rather detailed transient fields of velocities and other transport variables in full-scale process equipment operated under turbulent-flow conditions.

Commercial CFD software has become a reliable tool for carrying out simulations for laminar flows and—based on RANS—for turbulent flows. Practising engineers gradually have become convinced about the usefulness of RANS-based simulations. This review, however, emphasizes that CFD now has much more to offer. For practicing engineers confronted with mixing problems, it is

important to realize that CFD is not inherently restricted to just the average single-phase flow field, but gradually is becoming more and more capable of dealing with the details of turbulent eddies and two-phase flows. The performance of many physical operations and the yield and selectivity of many chemically reacting systems strongly depend on nonlinear interactions at the small scales of turbulent flows.

An example: Hollander *et al.* (2001a) nicely demonstrated how the strong inhomogeneities in stirred-tank flow result in unpredictable scale-up behaviour and that the impact of the detailed hydrodynamics and of the non-uniform spatial particle distribution on agglomeration rate is larger and more complex than usually assumed; their study once more illustrated the risks of scale-up on the basis of keeping a single non-dimensional number. Sophisticated CFD, especially on the basis of LES, offers an attractive alternative indeed.

Compared to RANS simulations, DNS and LES are much better geared to reproducing these small-scale processes. RANS simulations focus on the average flow only and by their nature just model the small scales rather rudimentarily. On the contrary, a DNS resolves all fluid motions and a LES resolves most part of the turbulence spectrum, i.e., all eddies larger than the grid cell size. While DNS nowadays can be used for turbulent flows at Reynolds numbers up to say 10,000 in simple geometries (channels, curved tubes) only, LES are quite feasible for complex geometries, certainly when LB techniques are adopted.

B. The Promises of Direct Numerical Simulations and Large Eddy Simulations

At the moment, DNS and LES for turbulent flows are still the playground of academic research groups. These groups are making substantial progress, however, in developing dedicated software for—and building up competence in—simulating multiphase flows, transport phenomena, many types of physical operations, and chemical reactions. Such dedicated software makes it possible to dig into the details of the mechanisms of a variety of flow and transport phenomena—often beyond the current capabilities of experimental techniques. That is why this review paper is an—admittedly provocative—plea for starting the exploitation of the advantages of DNS and LES.

An example: rather than linking average bubble size to just or essentially the (overall) power input of a particular vessel-impeller combination, dedicated CFD (preferably DNS and LES) allows for studying ('tracking') the response of bubble size to local and spatial variations in the turbulence levels in a stirred vessel. In this way, the validity of certain modeling assumptions may be affirmed or disproved. Particularly, effects of spatial variations in ε which

remain hidden in the traditional engineering techniques, may surface as a result of such dedicated CFD approaches. This type of dedicated CFD simulations offer a better and closer look into the details of flow and transport phenomena than experimental techniques which, e.g., still are not capable of delivering reliable high-resolution ε-values.

The advantage of LES over RANS-based simulations is that in the former approach modeling the effect of the unresolved scales of the flow is 'easier' and more straightforward, just because the SGS eddies are distinctly separated from the vessel boundary conditions and—as a result—their behavior is closer to the ideal of isotropy rendering universal turbulence modeling feasible. This makes the outcome of simulations less sensitive to deficiencies in turbulence modeling. This—along with the inherently transient character and the degree of detail of the simulations—turns LES highly suited as a base for simulating physical operations and chemical reactions carried out in stirred vessels. Whenever the performance of these processes is strongly dependent on turbulent mixing, the degree to which CFD simulations can be trusted depends on the ability to reproduce the complicated nonlinear interactions of flow and transport phenomena across the various turbulence scales. LES is then the CFD option to be recommended.

The present author even wonders whether we should not be satisfied with the gross predictions of the current RANS methods and turn to LES for the details of those single-phase and multiphase mixing processes which are dominated by the spatially distributed turbulence. It is really a valid question how long we should keep trying and improving the various RANS methods now the increased computer power brings the much more sophisticated LES within reach. The very nature of the RANS approach itself—particularly the basic assumptions as to averaging and the various modeling uncertainties as to turbulence and multiphase flow—may really set limits to its exploitation. The modest demands on computer resources RANS-based simulations require these days are no excuse in this respect.

In addition, DNS of turbulent flow in a periodic box offer interesting opportunities for studying in a fully resolved mode the intimate details of the flow field, its interaction with particles and the mutual interaction between particles (including particle–particle collisions and coalescence). Such simulations may yield new insights; see, e.g., Ten Cate *et al.* (2004) and Derksen (2006b). The same can be said about our understanding of particle–turbulence interactions in wall-bounded flows: this has increased due to Portela and Oliemans (2003) exploiting both DNS and LES and due to Ten Cate *et al.* (2004).

C. An Outlook

Nowadays, CFD research at academia is heavily engaged in attempts to include microscale transport phenomena and microscale processes in the dedicated codes under development with a view to reproduce such divergent processes as

blending, dissolution, crystallization, precipitation, coalescence and redispersion of bubbles and droplets, suspending solids, and chemical reactions. Essential physical challenges are in finding proper models for the details of the flow. In single-phase flows, we need better models for the unresolved contribution of microscale transport phenomena such as micromixing, while multiphase flow CFD looks for better models for the mutual interaction of turbulence and dispersed phase particles and for the interaction force(s) between the dispersed phase particles and the ambient continuous phase. 'The devil is in the detail' here fully applies.

In developing multiphase flow CFD and in combining CFD with population balances and various types of PDF approaches, one needs to keep the size of the computational job under control—in spite of the overwhelming growth in computational power (processor speed, memory, communication tools). This requires on the one hand efficient and effective numerical tools and on the other hand clever strategies for handling the enormous amounts of data. Local grid refinement techniques may be of great help in avoiding an unnecessary degree of detail.

The development of the above more dedicated LES and DNS is promoted by the introduction of LB techniques into the world of turbulent mixing simulations. LB techniques provide a viable alternative for the more classical FV solvers of the commercial CFD software, in particular in the context of parallel simulations on multiple processors. LB techniques are also inherently faster than FV techniques due to the locality of their operations. In addition, complex boundaries are easier to implement in the LB approach than with FV solvers.

Substantial improvements in LB techniques have been effected—in terms of immersed or embedded boundary methods for dealing with moving and curved boundaries (impeller blades, solid particles) and of grid refinement techniques—which have had a positive impact on the fast proliferation of dedicated CFD tools. Here, too, the details of the computational techniques do matter.

Finally, the large number of processors used in many of the parallel simulations cited is striking. It illustrates the enormous progress made in the size of the simulations academic groups have realized. The falling prices of such processors and the ease at which these can be combined into platforms for parallel simulations may have the effect that—just like in the past decade with RANS-based simulations—pretty soon industrial users can afford such dedicated and detailed simulations, both LES and DNS, and can benefit from their outcome in dealing with their commercial targets.

NOTATION

a	specific interface area
a_{ij}	anisotropy tensor, comprising, essentially, the turbulent stresses made nondimensional with the turbulent kinetic energy k

A	distance to origin in (A_3, A_2) plane
A_1, A_2, A_3	invariants of anisotropy tensor a_{ij}
c	concentration
c_s	*Smagorinsky* constant (in SGS modeling)
$C_{b\infty}$	coefficient in relation for local maximum bubble size $d_{b\infty}$
C_D	drag coefficient
C_{Dt}	drag coefficient in a free stream turbulence
C_μ	coefficient in model equation for v_t (in RANS models)
d_b	bubble size
$d_{b\infty}$	local maximum stable bubble size
D	diffusion (or dispersion) coefficient
D_{ij}	specific rate of production of turbulent stresses
D_k	specific rate of production of turbulent kinetic energy
D_ε	specific rate of production of ε (*Kolmogorov* eddies)
g	gravitational acceleration constant
$\mathbf{I}$	unity tensor
k	concentration of turbulent kinetic energy
k_l	mass transfer coefficient
k_{sgs}	turbulent kinetic energy contained in the SGS eddies
m_0	particle number concentration
n_b	particle number density
$n_{b\infty}$	local equilibrium number density
N	impeller speed (number of revolutions per unit of time)
p	pressure
$\tilde{p}$	pressure as resolved in LES
$\mathbf{P}$	average pressure (in RANS context)
P_{ij}	specific rate of production of turbulent stresses
P_k	specific rate of production of turbulent kinetic energy
$P\varepsilon$	specific rate of production of ε (*Kolmogorov* eddies)
q	specific heat production rate
r	specific rate of chemical reaction producing or consuming a particular species
$\hat{r}$	radial vector component
$\tilde{S}$	local resolved deformation rate (in LES)
S_g	source term in mass balance for gas phase (due to gas supply)
t	time
T	temperature
U_i U_j U_k	components of velocity vector $\mathbf{v}$ (in suffix notation)
$\overline{u_i u_j}$	average turbulent, or *Reynolds*, stresses
$\mathbf{u}$	gas velocity vector
$\mathbf{U_s}$	slip (or: relative) velocity vector
$\mathbf{v}$	fluid velocity vector

$\tilde{\mathbf{v}}$	fluid velocity vector as resolved in LES
$\mathbf{V}$	average fluid velocity vector (in RANS context)
V_b	bubble volume
$V_{b,in}$	bubble volume at position of gas supply
w	azimuthal component of velocity vector
x_i, x_k	spatial coordinate
X_Q	yield of product Q
$\hat{\mathbf{z}}$	vertical vector component

GREEK SYMBOLS

α	volume fraction of gas
β_0	agglomeration coefficient
δ_{ij}	*Kronecker* delta
Δ	grid spacing
ε	specific rate at which turbulent kinetic energy is dissipated (in the *Kolmogorov* eddies)
ε_{ij}	specific rate at which turbulent stresses are dissipated
η_B	*Batchelor* length scale (proportional to penetration depth for diffusion)
η_K	*Kolmogorov* length scale (smallest scale in turbulent flow)
κ	thermal conductivity coefficient
ν	kinematic viscosity coefficient
ν_e	effective SGS viscosity coefficient (in LES)
ν_t	turbulent viscosity coefficient (in RANS)
Π_{ij}	specific rate of production of turbulent stresses
Π_k	specific rate of production of turbulent kinetic energy
ρ	fluid density
ρ_l	liquid density
σ	interfacial tension
$\boldsymbol{\tau}$	shear stress tensor as resolved in LES
$\boldsymbol{\tau}'$	part of $\boldsymbol{\tau}$, see Eq. (3)
ω	effective break-up/agglomeration coefficient (a kind of relaxation parameter)
ω	vorticity
Ω	specific rate of destruction of ε

DIMENSIONLESS NUMBERS

Re	Reynolds number
Sc	Schmidt number

ABBREVIATIONS

ASM	Algebraic Stress Model
CDR	Convection-Diffusion-Reaction
CFD	Computational Fluid Dynamics
CSV	Cylindrical Stretched Vortex
CT	Computed Tomography
DNS	Direct Numerical Simulation
E	Engulfment
EDD	Engulfment-Deformation-Diffusion
FDF	Filtered Density Function
FV	Finite Volume
IEM	Interaction by Exchange with the Mean
ISAT	In situ Adaptive Tabulation
LB	Lattice-Boltzmann
LDA	Laser Doppler Anemometry
LDV	Laser Doppler Velocimetry
LDPE	Low Density Poly Ethylene
LES	Large Eddy Simulation
LGA	Lattice Gas Automaton
MC	Monte Carlo
MFR	Multiple Frames of Reference
NS	Navier–Stokes
PDF	Probability Density Function
QMOM	Quadrature Method of Moments
RANS	Reynolds Averaged Navier Stokes
RSM	Reynolds Stress Model
SGS	Sub Grid Scale
SDM	Sliding and Deforming Mesh
SM	Sliding Mesh
Sh	Shear
St	Strain
TVD	Total Variation Diminishing
VOF	Volume of Fluid

ACKNOWLEDGEMENTS

First of all, Dr. Jos J. Derksen of the Department of Multi-Scale Physics at Delft University of Technology is gratefully acknowledged for a fruitful long-time collaboration and for his critical review of the draft paper. The author is also indebted to all former PhD students of the ‘Kramers Laboratorium voor

Fysische Technologie' of Delft University of Technology for contributing through their PhD projects and theses to the development of the views and capabilities described in this chapter.

REFERENCES

Abbott, M. B., and Basco, D. R., "Computational Fluid Dynamics: An Introduction for Engineers". Longman Scientific & Technical, Harlow (UK) (1989).

Akiti, O., and Armenante, P. M. *AIChE J* **50**, 566–577 (2004).

Artoli, A. M., Hoekstra, A. G., and Sloot, P. M. A. *J. Mod. Phys. B* **17**(1–2), 95–98 (2003).

Bakker, A., "Hydrodynamics of stirred gas–liquid dispersions", Ph.D. Thesis, Delft University of Technology, Delft, Netherlands (1992).

Bakker, R. A., "Micromixing in chemical reactors: models, experiments and simulations", Ph.D. Thesis, Delft University of Technology, Delft, Netherlands (1996).

Bakker, A., and Fasano, J. B., "Time-Dependent, Turbulent Mixing and Chemical Reaction in Stirred Tanks, AIChE Symposium. Series No 299 90 71–78 (1993).

Bakker, A., LaRoche, R. D., Wang, M. H., and Calabrese, R. V. *Chem. Eng. Res. Des.* **75A**, 42–44 (1997).

Bakker, A., Oshinowo, L. M., and Marshall, E. M., "The Use of Large Eddy Simulation to Study Stirred Vessel Hydrodynamics". Proceedings of the 10th European Conference on Mixing, Delft, Netherlands, 247–254 (2000).

Bakker, A., and Oshinowo, L. M. *Chem. Eng. Res. Des.* **82**(A9), 1169–1178 (2004).

Bakker, A., and Van den Akker, H. E. A., "A Computational Study on Dispersing Gas in a Stirred Reactor". Proceedings of the 7th European Conference on Mixing, Brugue, Belgium 199–207. Also in: "Fluid mechanics of mixing: modelling, operations and experimental techniques", (R. King, Ed.) "Fluid Mechanics and its Applications", 10, 37–46. Kluwer Academic Publishers (1991).

Bakker, R. A., and Van den Akker, H. E. A. *Chem. Eng. Des.* **72A**, 733–738 (1994).

Bakker, A., and Van den Akker, H. E. A. *Chem. Eng. Res. Des.* **72A**, 583–593 (1994a).

Bakker, A., and Van den Akker, H. E. A. *Chem. Eng. Res. Des.* **72A**, 594–605 (1994b).

Bakker, R. A., and Van den Akker, H. E. A. *Chem. Eng. Sci.* **51**, 2643–2648 (1996).

Baldyga, J. *Chem. Eng. Sci.* **49**, 1985–2003 (1994).

Baldyga, J., and Bourne, J. R. *Chem. Eng. Commun.* **28**, 243–258 (1984a).

Baldyga, J., and Bourne, J. R. *Chem. Eng. Commun.* **28**, 259–281 (1984b).

Baldyga, J., and Henczka, M., Turbulent mixing and parallel chemical reactions in a pipe: application of a closure model, *Récents Progrès en Génie des Procédés* **11**, 341–348 (1997).

Bermingham, S. K., Kramer, H. J. M., and Van Rosmalen, G. M. *Comp. Chem. Eng.* **22**, 355–362 (1998).

Bourne, J. R., and Yu, S., "An Experimental Study of Micromixing Using Two Parallel Reactions". Proceedings of the 7th European Conference on Mixing, Brugues, Belgium, 67–75 (1991).

Bouwmans, I., "The blending of liquids in stirred vessels", Ph.D. Thesis, Delft University of Technology, Delft, Netherlands (1992).

Bouwmans, I., Bakker, A., and Van den Akker, H. E. A. *Chem. Eng. Res. Des.* **75A**, 777–783 (1997).

Brucato, A., Grisafi, F., and Montante, G. *Chem. Eng. Sci.* **53**, 3295–3314 (1998).

Bujalski, W., Jaworski, Z., and Nienow, A. W. *Chem. Eng. Res. Des.* **80**, 97–104 (2002).

Chen, S., and Doolen, G. D. *Ann. Rev. Fluid Mech* **30**, 329–364 (1998).

Colenbrander, G. W., "Experimental Findings on the Scale-Up Behaviour of the Drop Size Distribution of Liquid–Liquid Dispersions in Stirred Vessels". Proceedings of the 10th European Conference on Mixing, Delft, Netherlands, 173–180 (2000).

Curtis, J. S., and Van Wachem, B. *AIChE J* **50**, 2638–2645 (2004).
Derksen, J. J. *Chem. Eng. Res. Des.* **79A**, 824–830 (2001).
Derksen, J. J. *Lecture Notes Comput. Sci.* **2329**, 713–722 (2002a).
Derksen, J. J. *Flow Turbulence Combustion* **69**, 3–33 (2002b).
Derksen, J. J. *AIChE J* **49**, 2700–2714 (2003).
Derksen, J. J. *Chem. Eng. Res. Des.* **84**(A1), 38–46 (2006a).
Derksen, J. J., "Multi-scale simulations of stirred liquid–liquid dispersions". 12th European Conference on Mixing, Bologna, Italy, pp. 447–454 (2006b).
Derksen, J. J., Doelman, M. S., and Van den Akker, H. E. A. *Exp. Fluids* **27**, 522–532 (1999).
Derksen, J. J., Kooman, J. L., and Van den Akker, H. E. A., A parallel DNS implementation for confined swirling flow, *in* "HPCN Challenges in Telecomp and Telecom: Parallel Simulation of Complex Systems and Large-Scale Applications" (L. Dekker, *et al.,* Eds.), pp. 237–244. Elsevier, Amsterdam (1996).
Derksen, J. J., Kooman, J. L., and Van den Akker, H. E. A., "Parallel flow simulations by means of a lattice–Boltzmann scheme", In: B. Hertzberger, P. Sloot (Eds.), "High-Performance Computing and Networking", *Lecture Notes in Computer Science* **1225**, 524–530 (1997).
Derksen, J. J., and Van den Akker, H. E. A., "Large eddy simulation of stirred tank flow by means of a lattice-Boltzmann scheme", In: C. R. Kleijn, S. Kawano (Eds.), ASME Proceedings Volume PVP-377-2, ASME, 11–16 (1998).
Derksen, J. J., and Van den Akker, H. E. A. *AIChE J* **45**, 209–221 (1999).
Derksen, J. J., and Van den Akker, H. E. A. *AIChE J* **46**, 1317–1331 (2000).
Dimotakis, P. E. *Annu. Rev. Fluid Mech.* **37**, 329–356 (2005).
Distelhoff, M. F. W., Marquis, A. J., Nouri, J. M., and Whitelaw, J. H. *Can. J. Chem. Eng.* **75**, 641–652 (1997).
Ditl, P., and Rieger, F. *Chem. Eng. Progr.* **102**(1), 22–30 (2006).
Ducci, A., and Yianneskis, M. *Chem. Eng. Sci.* **61**, 2780–2790 (2006).
Eggels, J. G. M. *Int. J. Heat Fluid Flow* **17**(3), 307–323 (1996).
Eggels, J. G. M., and Somers, J. A. *Int. J. Heat Fluid Flow* **16**(5), 357–364 (1995).
Escudié, R., and Liné, A. *Chem. Eng. Sci.* **61**, 2771–2779 (2006).
Fox, R. O. *Rev. Inst. Franç. du Pétrole* **51**(2), 215–243 (1996).
Fox, R. O., "Computational Models for Turbulent reacting Flows". Cambridge University Press, Cambridge, UK (2003).
Frisch, U., "Turbulence, the Legacy of A. N. Kolmogorov". Cambridge University Press, Cambridge, UK (1995).
Frisch, U., Hasslacher, B., and Pomeau, Y. *Phys. Rev. Lett.* **56**, 1505–1508 (1986).
Gao, Z., and Min, J. *Chinese J. Chem. Eng.* **14**, 1–7 (2006).
Gao, Z., Min, J., Smith J. M., and Thorpe, R. B., "Large Eddy Simulation of Mixing Time in a Stirred Tank with Duals Rushton Turbines". 12th European Conference on Mixing, Bologna, Italy, pp. 431–438 (2006).
Gentric, C., Mignon, D., Bousquet, J., and Tanguy, P. A. *Chem. Eng. Sci.* **60**, 2253–2272 (2005).
Grenville, R. K., "Blending of viscous and pseudo-plastic fluids", Ph.D. Thesis, Cranfield Institute of Technology, Cranfield (UK) (1992).
Grenville, R. K., and Nienow, A. W., "Blending of miscible liquids," In: "NAMF Handbook of Industrial Mixing" (E. L. Paul, V. A. Atiemo-Obeng, and S. M. Kresta, Eds.), Wiley, Hoboken (NJ, USA) (2004).
Haam, S., Brodkey, R. S., and Fasano, J. B. *Ind. Eng. Chem. Res.* **31**, 1384–1391 (1992).
Hartmann, H., "Detailed simulations of liquid and liquid-solid mixing—turbulent agitated flow and mass transfer", Ph.D. Thesis, Delft University of Technology, Delft, Netherlands (2005).
Hartmann, H., Derksen, J. J., Montavon, C., Pearson, J., Hamill, I. S., and Van den Akker, H. E. A. *Chem. Eng. Sci.* **59**, 2419–2432 (2004a).
Hartmann, H., Derksen, J. J., and Van den Akker, H. E. A. *AIChE J* **50**, 2383–2393 (2004b).
Hartmann, H., Derksen, J. J., and Van den Akker, H. E. A. *Chem. Eng. Sci.* **61**, 3025–3032 (2006).

Harvey, P. S., and Greaves, M. *Trans. IChemE* **60**, 201–210 (1982).
Harvey, A. D., Lee, C. K., and Rogers, S. E. *AIChE J* **41**, 2177–2186 (1995).
Harvey, A. D., and Rogers, S. E. *AIChE J* **42**, 2701–2712 (1996).
Hasal, P., Montes, J. L., Boisson, H. C., and Fort, I. *Chem. Eng. Sci.* **55**, 391–401 (2000).
Hinze, J. O. *AIChE J* **1**, 289–295 (1955).
Hirt, C. W., and Nichols, B. D. *J. Comput. Phys.* **39**, 201–225 (1981).
Hoekstra, A. J., "Gas flow field and collection efficiency of cyclone separators", Ph.D. Thesis, Delft University of Technology, Delft, Netherlands (2000).
Hollander, E. D., "Shear induced agglomeration and mixing", Ph.D. Thesis, Delft University of Technology, Delft, Netherlands (2002).
Hollander, E. D, Derksen, J. J., Bruinsma, O. S. L., Van Rosmalen, G. M., and Van den Akker, H. E. A., "A Numerical Investigation into the Influence of Mixing on Orthokinetic Agglomeration". Proceedings of the 10th European Conference on Mixing, Delft, Netherlands, 221–230 (2000).
Hollander, E. D., Derksen, J. J., Portela, L. M., and Van den Akker, H. E. A. *AIChE J* **47**, 2425–2440 (2001a).
Hollander, E. D., Derksen, J. J., Bruinsma, O. S. L., Van den Akker, H. E. A., and Van Rosmalen, G. M. *Chem. Eng. Sci.* **56**, 2531–2541 (2001b).
Hollander, E. D., Derksen, J. J., Kramer, H. M. J., Van Rosmalen, G. M., and Van den Akker, H. E. A. *Powder Technol.* **130**, 169–173 (2003).
Holmes, D. B., Voncken, R. M., and Dekker, J. A. *Chem. Eng. Sci.* **19**, 201–208 (1964).
Hoogendoorn, C. J., and Den Hartog, A. P. *Chem. Eng. Sci.* **22**, 1689–1699 (1967).
Hristov, H. V., Mann, R., Lossev, V., and Vlaev, S. D. *Trans. IChemE, Food Bioproducts Process* **82**(C1), 21–34 (2004).
Issa, R., and Gosman, A. D., "The Computation of Three-Dimensional Turbulent Two-Phase Flow in Mixer Vessels". Proc. 2nd Int. Conf. Num. Meth. Lam. Turb. Flows, Venice, Italy (1981).
Jahoda, M., Moštěk, M., Kukuková, A., and Machoň, V., "CFD Modelling of Liquid Homogenisation in Stirred Tanks With One and Two Impellers Using Large Eddy Simulation". 12th European Conference on Mixing, Bologna, Italy, pp. 455–462 (2006).
Jaworski, Z., Bujalski, W., Otomo, N., and Nienow, A. W. *Chem. Eng. Res. Des.* **78**, 327–333 (2000).
Kandhai, D., Derksen, J. J., and Van den Akker, H. E. A. *AIChE J* **49**, 1060–1065 (2003).
Khopkar, A. R., Rammohan, A. R., Ranade, V. V., and Dudukovic, M. P. *Chem. Eng. Sci.* **60**, 2215–2229 (2005).
Khopkar, A. R., Kasat, G. R., Pandit, A. B., and Ranade, V. V. *Chem. Eng. Sci.* **61**, 2921–2929 (2006).
Kramers, H., Baars, G. M., and Knoll, W. H. *Chem. Eng. Sci.* **2**, 35–42 (1953).
Kresta, S. M., and Brodkey, R. S., Turbulence in mixing applications, Ch.2, In: Paul, E. L., Atiemo-Obeng, V. A., Kresta, S. M. (Eds.),"NAMF Handbook of Industrial Mixing", Wiley, Hobken (NJ, USA) (2004).
Laakkonen, M., Alopeus, V., and Aittamaa, J. *Chem. Eng. Sci.* **61**, 218–228 (2006).
Lance, M., Marié, J. L., and Bataille, J. *J. Fluids Eng.* **113**, 295–300 (1991).
Lane, G. L., Schwarz, M. P., and Evans, G. M., "Modelling of the Interaction Between Gas and Liquid in Stirred Vessels". Proceedings of the 10th European Conference on Mixing, Delft, Netherlands, 197–204 (2000).
Lapin, A., Müller, D., and Reuss, M. *Ind. Eng. Chem. Res.* **43**, 4647–4656 (2004).
Lathouwers, D., "Modelling and simulation of turbulent bubbly flow", Ph.D. Thesis, Delft University of Technology, Delft, Netherlands (1999).
Lathouwers, D., and Van den Akker, H. E. A., "A numerical method for the solution of two-fluid model equations". Proceedings of the Fluids Eng. Div. 1996 Summer Meeting, San Diego (CA, USA), ASME, New York (USA), Vol. 1, 121–126 (1996).
Lee, K. C., "An experimental investigation of the trailing vortex structure and mixing characteristics of mixing vessels", Ph.D. Thesis, King's College, London, (UK) (1995).

Liu, S. *Chem. Eng. Sci.* **54**, 873–891 (1999).
Lo, S., "Application of population balance to CFD modelling of gas–liquid reactors". Conference on "Trends in Numerical and Physical Modelling for Industrial Multiphase Flows", Cargèse, Corse 27–29 September (2000).
Lu, Z., Liao, Y., Qian, D., McLaughlin, J. B., Derksen, J. J., and Kontomaris, K. *J. Comput. Physics* **181**, 675–704 (2002).
Lumley, J. *Adv. Appl. Mech.* **24**, 123–176 (1978).
Luo, J. Y., Gosman, A. D., Issa, R. I., Middleton, J. C., and Fitzgerald, M. K. *Trans. IChemE.* **71A**, 342–344 (1993).
Luo, J. Y., Issa, R. I., and Gosman, A. D. *IChemE Symp. Ser.* **136**, 549–556 (1994).
Luo, H., and Svendsen, H. F. *AIChE J* **42**, 1225–1233 (1996).
Marchisio, D. L., and Barresi, A. A. *Chem. Eng. Sci.* **58**, 3579–3587 (2003).
Marchisio, D. L., Pikturna, J. T., Fox, R. O., Vigil, R. D., and Barresi, A. A. *AIChE J* **49**, 1266–1276 (2003).
Marshall, E., and Bakker, A., "Computational Fluid Mixing". Fluent Inc. Lebanon, NH; also as Ch. 5 In: Paul, E. L., Atiemo-Obeng, V. A., Kresta, S. M. (Eds.), "NAMF Handbook of Industrial Mixing", Wiley, Hoboken (NJ, USA) (2004).
Mason, P. J., and Callen, N. S. *J. Fluid Mech.* **162**, 439–462 (1986).
McNamara, G., and Zanetti, G. *Phys. Rev. Lett.* **61**, 2332–2335 (1988).
Menter, F. R. *AIAA J* **32**(8), 269–289 (1994).
Micale, G., Montante, G., Grisafi, F., Brucato, A., and Godfrey, J. *Chem. Eng. Res. Des.* **78**, 435–444 (2000).
Micale, G., Grisafi, F., Rizzuti, L., and Brucato, A. *Chem. Eng. Res. Des.* **82**, 1204–1213 (2004).
Micheletti, M., Baldi, S., Yeoh, S. L., Ducci, A., Papadakis, G., Lee, K. C., and Yianneskis, M. *Chem. Eng. Res. Des.* **82**, 1188–1198 (2004).
Middleton, J. C., Pierce, F., and Lynch, P. M. *Chem. Eng. Res. Des.* **64**, 18–22 (1986).
Mittal, R., and Iaccarino, G. *Annu. Rev. Fluid Mech.* **37**, 239–261 (2005).
Moin, P., and Kim, J., *Sci. Am.*, **January** 46–52 (1997).
Montante, G., Micale, G., Brucato, A., and Magelli, F., "CFD Simulation of Particle Distribution in a Multiple-Impeller High-Aspect-Ratio Stirred Vessel". Proceedings of the 10th European Conference on Mixing, Delft, Netherlands, 125–132 (2000).
Montante, G., and Magelli, F. *Chem. Eng. Res. Des.* **82**, 1179–1187 (2004).
Montante, G., and Magelli, F. *Int. J. Comp. Fluid Dynam.* **19**, 253–262 (2005).
Montante, G., Bakker, A., Paglianti, A., and Magelli, F. *Chem. Eng. Sci.* **61**, 2807–2814 (2006).
Mumtaz, H. S., Hounslow, M. J., Seaton, M. J., and Paterson, W. R. *Chem. Eng. Res. Des.* **75**, 152–159 (1997).
Murthy, J. Y., Mathur, S. R., and Choudhury, D. *IChemE Symp.Ser.* **136**, 341–345 (1994).
Myers, K. J., Ward, R. W., and Bakker, A. *ASME J. Fluids Eng.* **119**, 623–632 (1997).
Nienow, A. W. *Chem. Eng. Sci.* **52**, 2557–2565 (1997).
Nikiforaki, L., Montante, G., Lee, K. C., and Yianneskis, M. *Chem. Eng. Sci.* **58**, 2937–2949 (2002).
Oey, R. S., Mudde, R. F., and Van den Akker, H. E. A. *AIChE J* **49**, 1621–1636 (2003).
Osman, J. J., and Varley, J. *IChemE Symp.Ser.* **146**, 15–22 (1999).
Ottino, J. M. *Chem. Eng. Sci.* **35**, 1377–1391 (1980).
Patankar, S. V., "Numerical Heat Transfer and Fluid Flow". Hemisphere Publishing Corporation, New York (USA) (1980).
Patterson, G. K., "Modelling of turbulent reactors," Ch. 3, In: "Mixing of Liquids by Mechanical Agitation". (J. J. Ulbrecht and G. K. Patterson, Eds.), Gordon and Breach Science Publishers, New York (USA) (1985).
Patterson, G. K., Paul, E. L., Kresta, S. M., and Etchells, A. W. III., "Mixing and chemical reactions," Ch. 13, In: "NAMF Handbook of Industrial Mixing" (E. L. Paul, V.A. Atiemo-Obeng, and S. M. Kresta, Eds.), Wiley, Hoboken (USA) (2004).

Paul, E. L., Atiemo-Obeng, V. A., and Kresta, S. M., "NAMF Hand book of Industrial Mixing". Wiley, Hoboken (USA) (2004).
Pericleous, K. A., and Patel, M. K. *Physico Chem. Hydrodynam* **8**, 105–123 (1987).
Pinelli, D., Nocentini, M., and Magelli, F. *Chem. Eng. Commun.* **188**, 91–107 (2001).
Placek, J., and Tavlarides, L. *AIChE J* **31**, 1113–1120 (1985).
Placek, J., Tavlarides, L., Smith, G. W., and Fort, I. *AIChE J* **32**, 1771–1785 (1986).
Pope, S. B. *Prog. Energy Combust. Sci.* **11**, 119–192 (1985).
Portela, L. M., and Oliemans, R. V. A. *Int. J. Numer. Meth. Fluids* **43**, 1045–1065 (2003).
Praturi, A. K., and Brodkey, R. S. *J. Fluid Mech.* **89**, 251–272 (1978).
Procházka, J., and Landau, J. *Coll. Czech. Chem. Commun* **26**, 2961–2973 (1961).
Ranade, V. V., "Computational Flow Modeling for Chemical Reactor Engineering," Volume 5 of Process Systems Engineering (G. Stephanopoulos and J. Perkins, Eds.), Academic Press, San Diego (CA, USA) (2002).
Ranade, V. V., Bourne, J. R., and Joshi, J. B. *Chem. Eng. Sci.* **46**, 1883–1893 (1991).
Ranade, V. V., and Dommeti, S. M. S. *Chem. Eng. Res. Des.* **74A**, 476–484 (1996).
Ranade, V. V., Joshi, J. B., and Marathe, A. G. *Chem. Eng. Commun.* **81**, 225–248 (1989).
Ranade, V. V., and Van den Akker, H. E. A. *Chem. Eng. Sci.* **49**, 5175–5192 (1994).
Ranz, W. E. *AIChE J* **25**, 41–47 (1979).
Revstedt, J., Fuchs, L., and Trägårdh, Ch. *Chem. Eng. Sci.* **53**, 4041–4053 (1998).
Revstedt, J., Fuchs, L., Kovács, T., and Trägårdh, Ch. *AIChE J* **46**, 2373–2382 (2000).
Revstedt, J., and Fuchs, L. *Chem. Eng. Technol.* **25**, 443–446 (2002).
Rielly, C. D., and Marquis, A. J. *Chem. Eng. Sci.* **56**, 2475–2493 (2001).
Rietema, K., and Van den Akker, H. E. A. *Int. J. Multiphase Flow* **9**, 21–36 (1983).
Rodi, W.,"Turbulence models and their application in hydraulics—a state of the art review", International Association for Hydraulic Research, Delft (NL), reprinted in 1984 (1984).
Rohde, M., "Extending the Lattice-Boltzmann method—novel techniques for local grid refinement and boundary conditions", Ph.D. Thesis, Delft University of Technology, Delft, Netherlands (2004).
Rohde, M., Derksen, J. J., and Van den Akker, H. E. A., *Phys. Rev. E* **65**, Paper No. 056701 (2002).
Rohde, M., Kandhai, D., Derksen, J. J., and Van den Akker, H. E. A., *Phys. Rev. E* **67**, Paper No. 066703 (2003).
Rohde, M., Kandhai, D., Derksen, J. J., and Van den Akker, H. E. A. *Int. J. Numer. Meth. Fluids* **51**(7), 439–468 (2006).
Roušar, I., and Van den Akker, H. E. A., "LDA Measurements of Liquid Velocities in Sparged Agitated Tanks with Single and Multiple Rushton Turbines". 8th European Conference on Mixing, Cambridge, UK *IChemE Symp. Ser.*, **136**, 89–96 (1994).
Roussinova, V., Kresta, S. M., and Weetman, R. *Chem. Eng. Sci.* **58**, 2297–2311 (2003).
Rushton, J. H., Costich, E. W., and Everett, H. J. *Chem. Eng. Progr* **46**, 395–404 467–476 (1950).
Ruszkowski, S., "A Rational Method for Measuring Blending Performance, and Comparison of Different Impeller Types". Proceedings of the 8th European Conference on Mixing, Cambridge, UK, pp. 283–291 (1994).
Sano, Y., and Usui, H. *J. Chem. Eng Japan* **18**, 47–52 (1985).
Schäfer, M., Höfken, M., and Durst, F. *Chem. Eng. Res. Des.* **75A**, 729–736 (1997).
Schäfer, M., Yianneskis, M., Wächter, P., and Durst, F. *AIChE J* **44**, 1233–1246 (1998).
Schulze, K., Ritter, J., and Kraume, M., "Investigations of Local Drop Size Distributions and Scale-Up in Stirred Liquid–Liquid Dispersions". Proceedings of the 10th European Conference on Mixing, Delft, Netherlands, 181–188 (2000).
Seckler, M. M., Bruinsma, O. S. L., and Van Rosmalen, G. M. *Chem. Eng. Commun.* **135**, 113–131 (1995).
Shaw, C. T., "Using Computational Fluid Dynamics". Prentice Hall International Ltd, Hemel Hempstead (UK) (1992).

Shyy, W. *Adv. Heat Transfer* **24**, 191–275 (1994).
Smagorinsky, J. *Monthly Weather Rev.* **91**, 99–164 (1963).
Somers, J. A. *Appl. Sci. Res.* **51**, 127–133 (1993).
Sommerfeld, M., and Decker, S. *Chem. Eng. Technol.* **27**(3), 215–224 (2004).
Stekelenburg, A. J. C., Van der Hagen, T. H. J. J., and Van den Akker, H. E. A. *Int. J. Num. Meth. Heat Fluid Flow* **4**, 143–158 (1994).
Succi, S., "The Lattice Boltzmann Equation for Fluid Dynamics and Beyond". Oxford University Press, New York (USA) (2001).
Ten Cate, A., "Turbulence and particle dynamics in dense crystal slurries—a numerical study by means of lattice-Boltzmann simulations", Ph.D. Thesis, Delft University of Technology, Delft, Netherlands (2002).
Ten Cate, A., Bermingham, S. K., Derksen, J. J., and Kramer, H. M. J., Compartmental Modeling of a 1,100 L Crystallizer Based on Large Eddy Flow Simulation". Proceedings of the 10th European Conference on Mixing, Delft, Netherlands, 255–264 (2000).
Ten Cate, A., Derksen, J. J., Kramer, H. J. M., Van Rosmalen, G. M., and Van den Akker, H. E. A. *Chem. Eng. Sci.* **56**, 2495–2509 (2001).
Ten Cate, A., Derksen, J. J., Portela, L. M., and Van den Akker, H. E. A. *J. Fluid Mech.* **519**, 233–271 (2004).
Tennekes, H., and Lumley, J. L., "A First Course in Turbulence". MIT Press, Cambridge (MA, USA) (1972).
Thornock, J. N., and Smith, P. J. *WIT Trans. Built Environ* **84**, 573–583 (2005).
Trägårdh, Ch., "A Hydrodynamic Model for the Simulation of an Aerated Agitated Fed-Batch Fermentor". Proceedings of the 2nd International Conference on Bioreactor Fluid Dynamics, Cambridge, UK 117–134 (1988).
Tsouris, C., and Tavlarides, L. L. *AIChE J* **40**, 395–406 (1994).
Van den Akker, H. E. A.,"On Status and Merits of Computational Fluid Dynamics". In: Nienow, A. W. (Ed.), Proceedings of the 4th International Conference on Bioreactor and Bioprocess Fluid Dynamics, BHR, Edinburgh, UK 407–432 (1997).
Van den Akker, H. E. A. *ERCOFTAC Bull* **36**, 30–33 (1998).
Van den Akker, H.E.A., "Momentum Equations in Dispersed Two-Phase Flows". In: Cheremisinoff, N.P. (Ed.), Encyclopedia of Fluid Mechanics, Gulf Publishing Company, Houston (TX, USA), Vol. 3, Chapter 15, 371–400 (1986).
Van den Akker, H. E. A., "Computational fluid dynamics: more than a promise to chemical reaction engineering". Plenary paper presented at CHISA, Prague, CZ Paper #1270 (2000).
Van Leeuwen, M. L. J., "Precipitation and mixing", Ph.D. Thesis, Delft University of Technology, Delft, Netherlands (1998).
Van Leeuwen, M. L. J., Bruinsma, O. S. L., and Van Rosmalen, G. M. *Chem. Eng. Sci.* **51**, 2595–2600 (1996).
Van Santen, H., Lathouwers, D., Kleijn, C. R., and Van den Akker, H. E. A., "Influence of segregation on the efficiency of finite volume methods for the incompressible Navier–Stokes equations". Proceeding of the Fluids Eng. Div. 1996 Summer Meeting, San Diego (CA, USA), ASME, New York (USA), Vol. 3, 151–158 (1996).
Van Vliet, E., "Turbulent reactive mixing in process equipment", Ph.D. Thesis, Delft University of Technology, Delft, Netherlands (2003).
Van Vliet, E., Derksen, J. J., and Van den Akker, H. E. A., "Modelling of Parallel Competitive Reactions in Isotropic Homogeneous Turbulence Using a Filtered Density Function Approach for Large Eddy Simulations". Proc. PVP01 3rd Int. Symp. on Comput. Techn. for Fluid/Thermal/Chemical Systems with Industrial Appl., Atlanta, GE, USA (2001).
Van Vliet, E., Derksen, J. J., and Van den Akker, H. E. A., "A numerical study of a low-density polyethylene tubular reactor using a 3-D FDF/LES approach", AIChE 2004 Annual Mtg., Austin, TX, USA (2004).
Van Vliet, E., Derksen, J. J., and Van den Akker, H. E. A. *AIChE J* **51**, 725–739 (2005).

Van Vliet, E., Derksen, J. J., and Van den Akker, H. E. A., "Numerical Study on the Turbulent Reacting Flow in the Injector Region of an LDPE Tubular Reactor". Proceedings of the 12th European Conference on Mixing, Bologna, Italy, pp. 719–726 (2006).
Van Wageningen, W. F. C., Kandhai, D., Mudde, R. F., and Van den Akker, H. E. A. *AIChE J* **50**, 1684–1696 (2004).
Venneker, B. C. H., Turbulent flow and gas dispersion in stirred vessels with pseudo plastic fluids", Ph.D. Thesis, Delft University of Technology, Delft, Netherlands (1999).
Venneker, B. C. H., Derksen, J. J., and Van den Akker, H. E. A. *AIChE J* **48**, 673–685 (2002).
Voncken, R. M., Holmes, D. B., and Den Hartog, H. W. *Chem. Eng. Sci.* **19**, 209–213 (1964).
Von Smoluchowski, M. *Phys. Chem.* **92**, 129–156 (1917).
Vuik, C., "Fast iterative solvers for the discretized incompressible Navier–Stokes equations", Delft University of Technology, TMI TR93-98 (1993).
Wang, T., Wang, J., and Jin, Y. *AIChE J* **52**, 125–140 (2006).
Wei, H., and Garside, J. *Chem. Eng. Res. Des.* **75**, 219–227 (1997).
Westerterp, K. R., Van Dierendonck, L. L., and De Kraa, J. A. *Chem. Eng. Sci.* **18**, 157–176 (1963).
Wilcox, D. C., "Turbulence Modelling for CFD". DCW Industries Inc., La Canada (CA) (1993).
Wu, H., and Patterson, G. K. *Chem. Eng. Sci.* **44**, 2207–2221 (1989).
Yeoh, S. L., Papadakis, G., and Yianneskis, M. *Chem. Eng. Res. Des.* **82**(A7), 834–848 (2004a).
Yeoh, S. L., Papadakis, G., Lee, K. C., and Yianneskis, M. *Chem. Eng. Technol.* **27**, 257–263 (2004b).
Yeoh, S. L., Papadakis, G., and Yianneskis, M. *Chem. Eng. Sci.* **60**, 2293–2302 (2005).
Yianneskis, M., Popiolek, Z., and Whitelaw, J. H. *J. Fluid Mech.* **175**, 537–555 (1987).
Zwietering, Th. N. *Chem. Eng. Sci.* **8**, 244–253 (1958).